

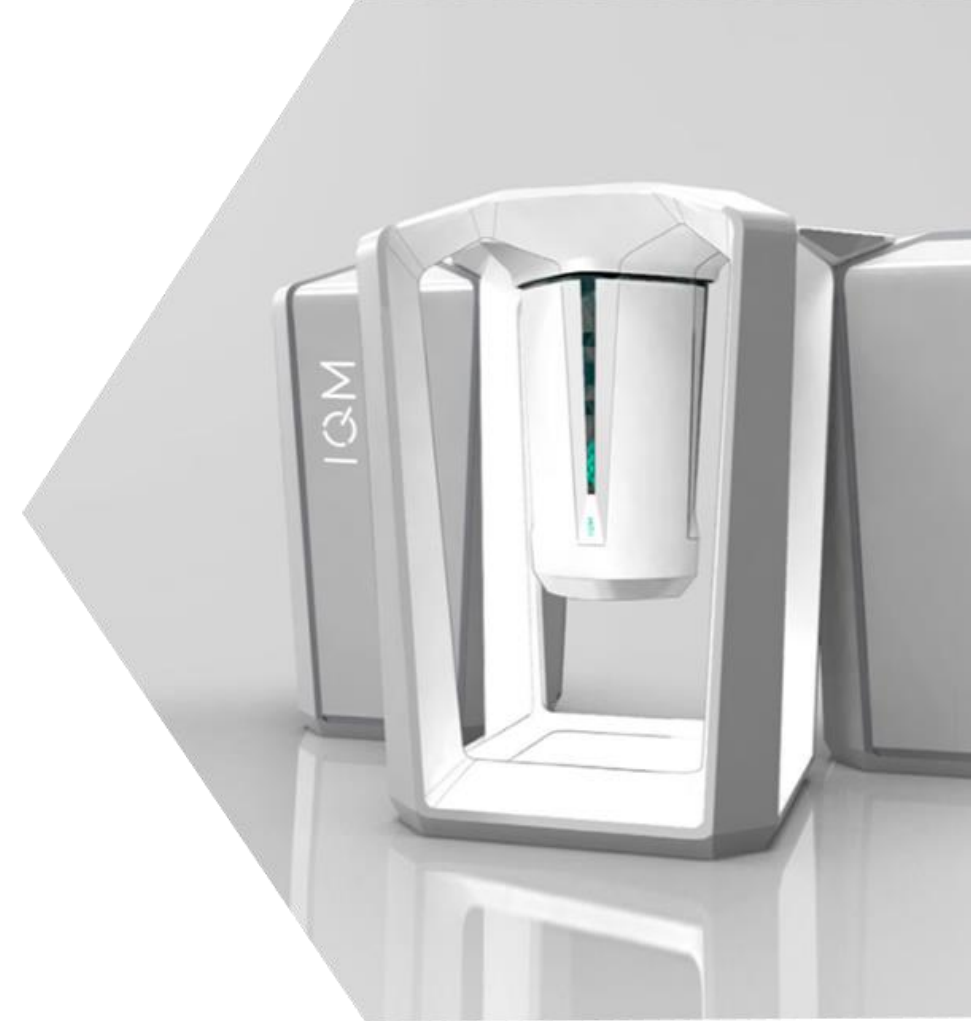


WE BUILD QUANTUM COMPUTERS

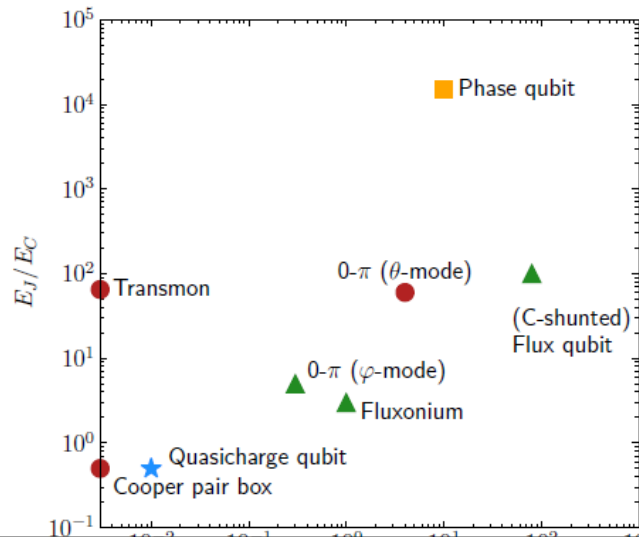
Jan Goetz

Lecture notes on PHYS-C0254 Quantum Circuits

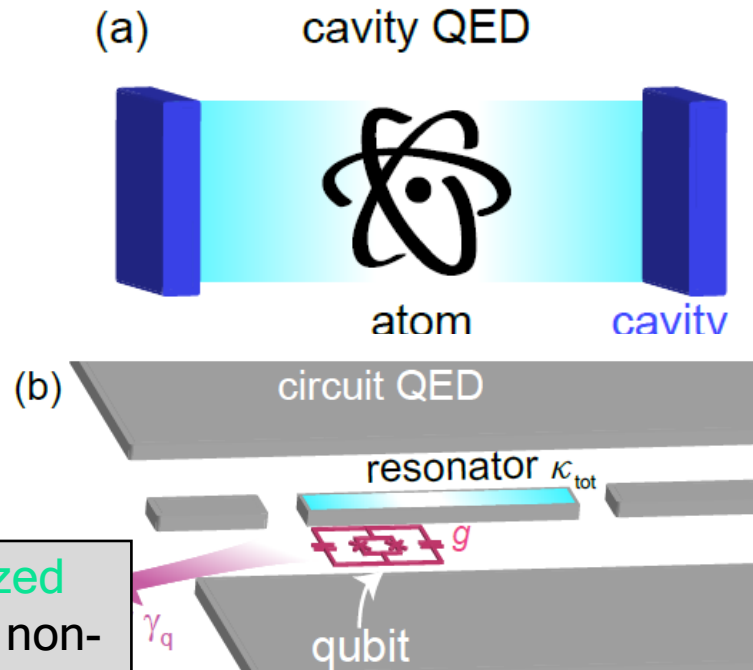
[www.meetiqm.com](http://www.meetiqm.com)



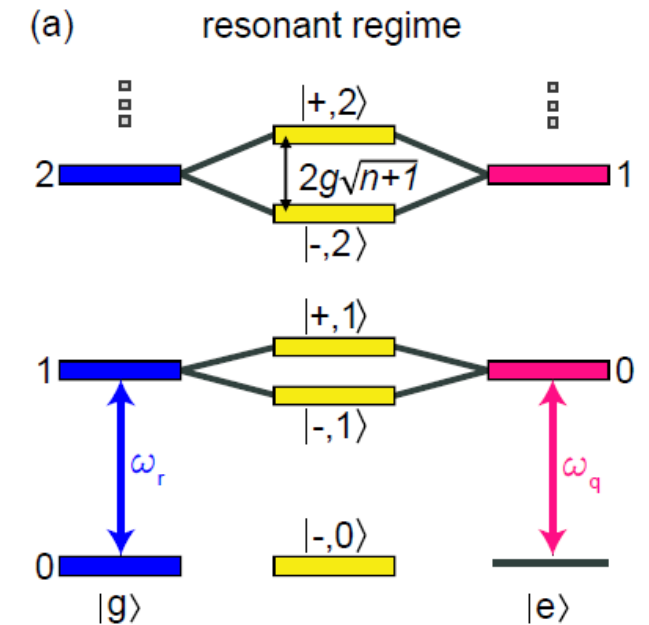
# Short recap from last week



Superconducting circuits have **quantized energy levels**. Josephson junctions are non-linear elements which allow us to make the energy spacing **non-equidistant**. We can create a situation where all but 2 energy levels can be ignored creating effectively a quantum two-level system, i.e., a qubit.



Key takeaway:  
Superconducting circuits follow the physics of **quantum optics** and can reach **parameter regimes** that are unreachable in nature.



Key takeaway: In the **dispersive regime** of the Jaynes-Cummings model, resonators can be used for **qubit readout**.

# Agenda for lectures 7-12

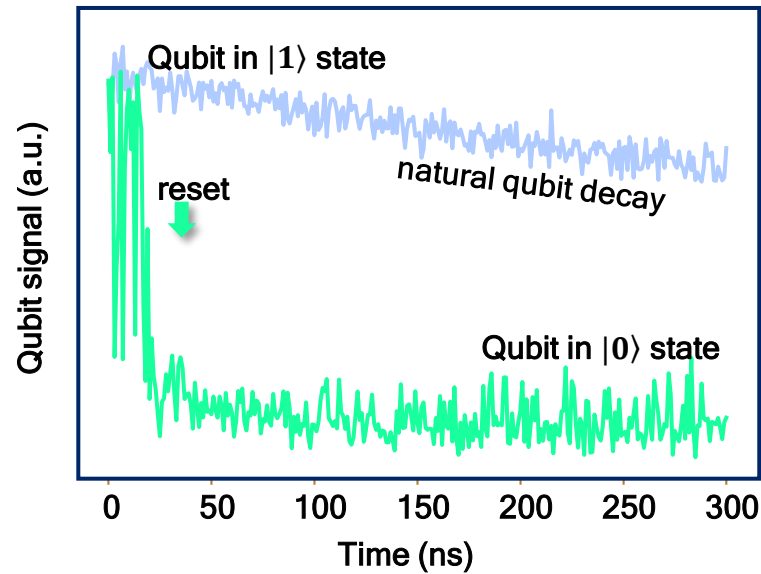
7. Quantization of electrical networks
  - a. Harmonic oscillator: Lagrangian, eigenfrequency
  - b. Transfer step: LC oscillator, Legendre transform to Hamiltonian
  - d. Quantization of oscillators
8. Superconducting quantum circuits
  - a. Qubits: Transmon qubit, Charge qubit, Flux qubit 1<sup>st</sup> DiVincenzo criteria
  - b. Circuit-QED: Rabi model
  - c. Rotating Wave approximation: Jaynes-Cummings model
9. Single-qubit operations:
  - a. Initialization 2<sup>nd</sup> DiVincenzo criteria
  - b. Readout 5<sup>th</sup> DiVincenzo criteria
  - c. Control: T1, T2 measurements, Randomized benchmarking 3<sup>rd</sup> DiVincenzo criteria
10. Two-qubit operations: Architectures for 2-qubit gates 4<sup>th</sup> DiVincenzo criteria
  - a. iSWAP
  - b. cPhase
  - c. cNot
  - d. maybe: Google supremacy experiment
11. Quantum algorithms
  - a. VQE
  - b. Grover search
12. Challenges in quantum computing
  - a. Scaling
  - b. SW-HW gap
  - c. Error-correction

# Agenda for today

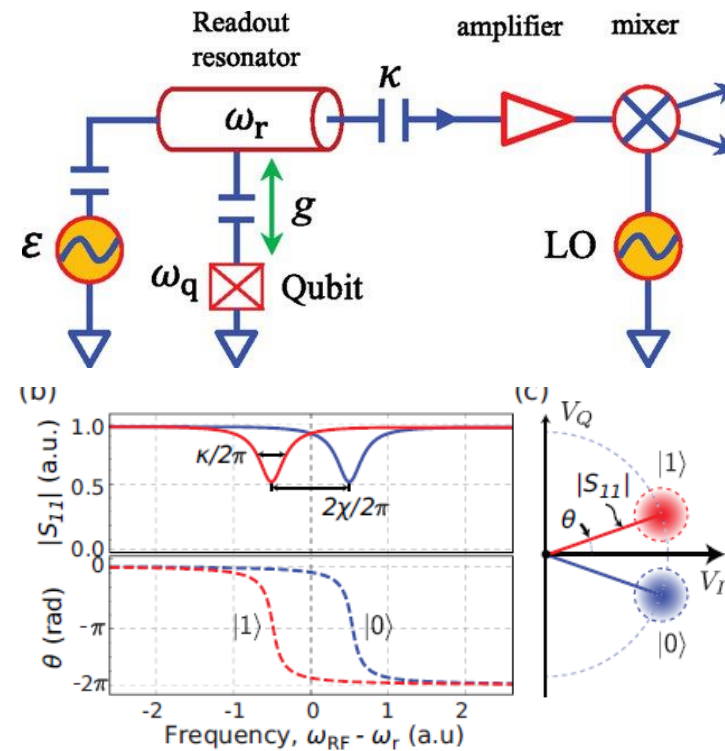
## 9. Single-qubit operations:

- Initialization **2<sup>nd</sup> DiVincenzo criteria**
- Readout **5<sup>th</sup> DiVincenzo criteria**
- Control: T1, T2 measurements, Randomized benchmarking **3<sup>rd</sup> DiVincenzo criteria**

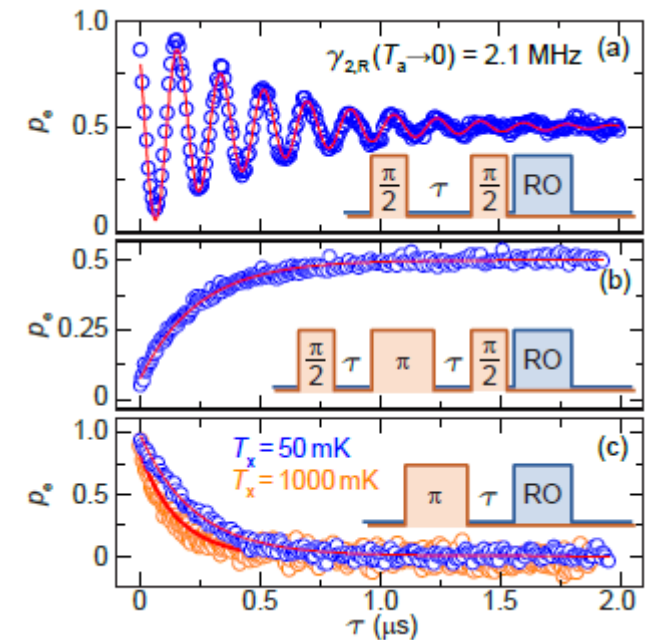
a.



b.



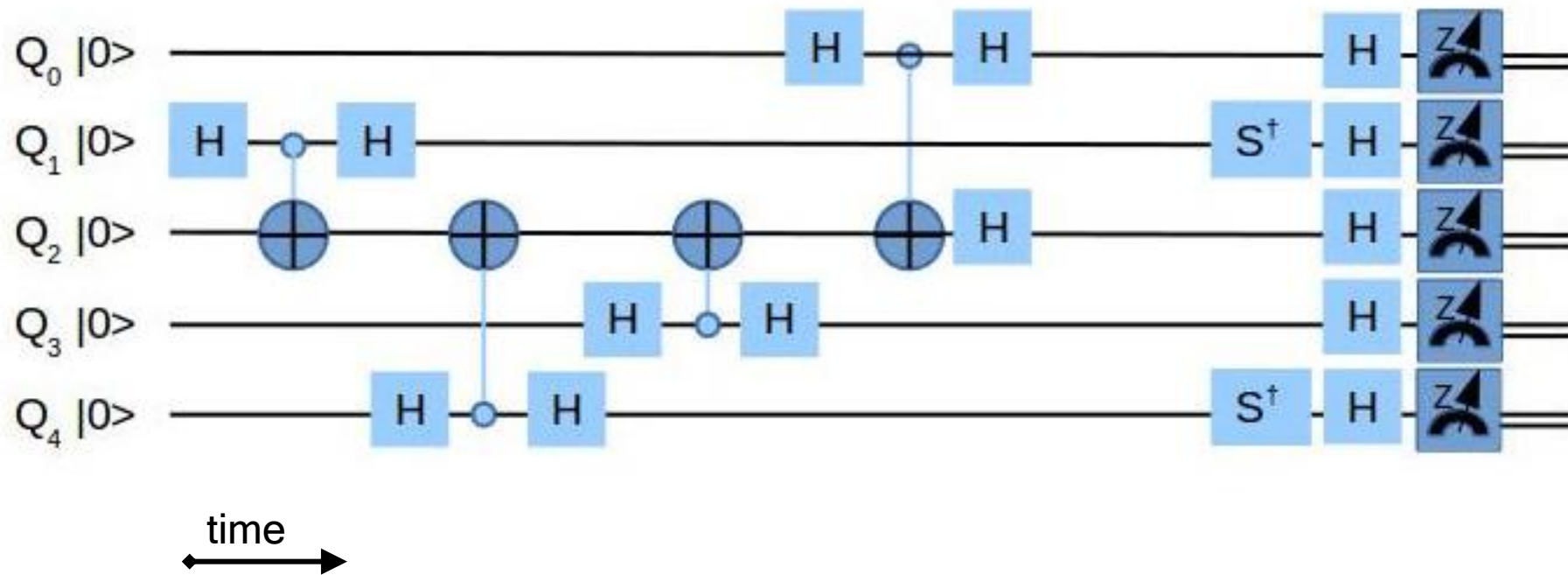
c.



# General approach: Initialization, gates, readout

- To execute quantum algorithms, one needs three main operations: **initialization, gates, readout**.
- Usually one wants to **isolate** the quantum circuits as much as possible, however, the above operations need a certain **interaction**.
- Due to noise and other parasitic couplings, the operations we perform are **never ideal** and we will always make errors.

# Short intro: The basic elements of quantum algorithms



# General approach: Initialization

- To **start a computation**, it is necessary that all registers are in a well-known state, typically the 0-state.
- For experimental implementation, **thermal noise** always drives us out of equilibrium when approaching the 0-state.
- We can compensate this by **actively cooling** or used more advanced feedback or pulse schemes.

# Short recap: the qubit state

We can effectively describe our non-linear superconducting circuit as a quantum 2-level system following the Hamiltonian

$$\mathcal{H}_q = \frac{\omega_q}{2} \hat{\sigma}_z$$

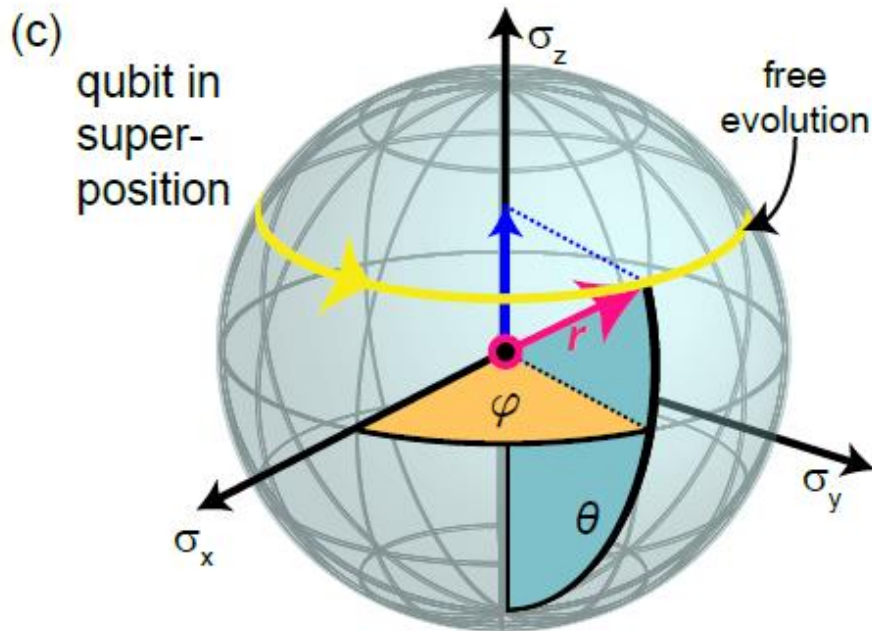
In the absence of decoherence, we describe the qubit dynamics by a time evolution of the Bloch vector

$$|\Psi\rangle = \cos \frac{\theta}{2} |g\rangle + e^{i\varphi} \sin \frac{\theta}{2} |e\rangle = \begin{pmatrix} \cos \frac{\theta}{2} \\ e^{i\varphi} \sin \frac{\theta}{2} \end{pmatrix}$$

This allows us to define qubit operations as rotations with certain angles carried out on the qubit state in the basis

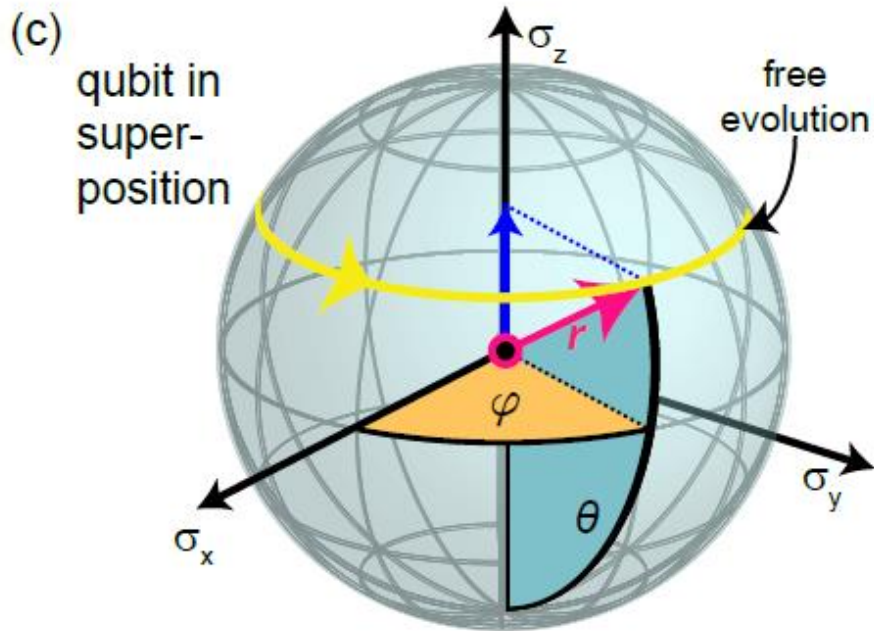
$$|e\rangle = \begin{pmatrix} 1 \\ 0 \end{pmatrix}, \quad |g\rangle = \begin{pmatrix} 0 \\ 1 \end{pmatrix}.$$

Initialization means bringing the qubit controlled into the ground state.





# In real life: thermal states



In an experimental setup, circuits are never isolated but coupled to an environment, e.g., the silicon substrate. Hence, they will end up in a thermal state.

The probability to find the circuit in a thermally excited state is given by the Maxwell-Boltzmann distribution

$$P_{|i\rangle} = \frac{1}{Z} g_i \exp(-E_i/k_B T)$$

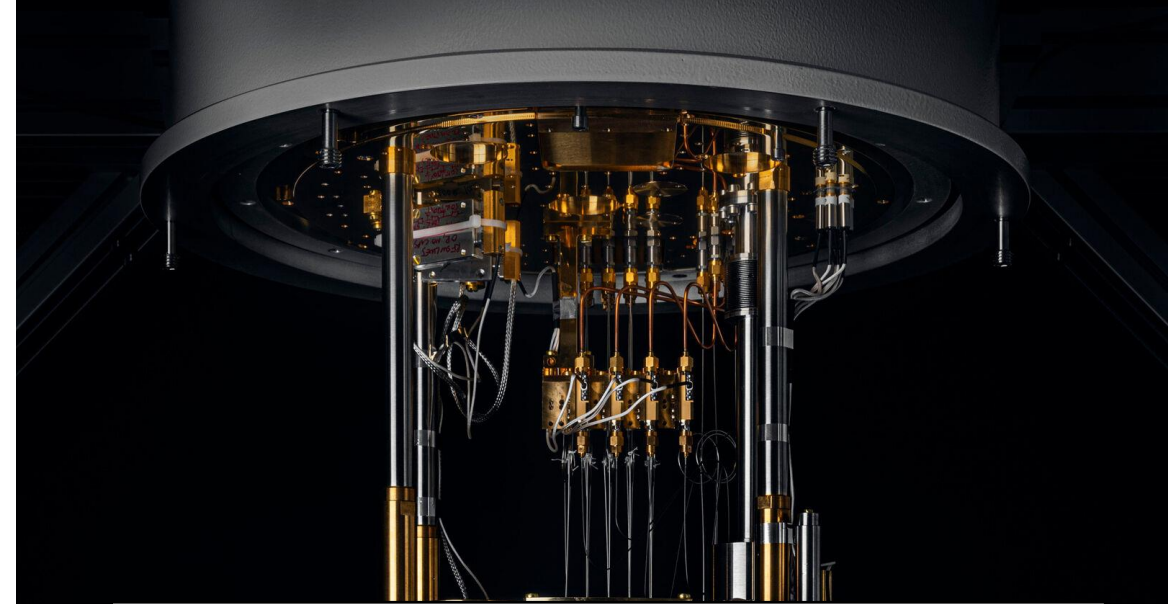
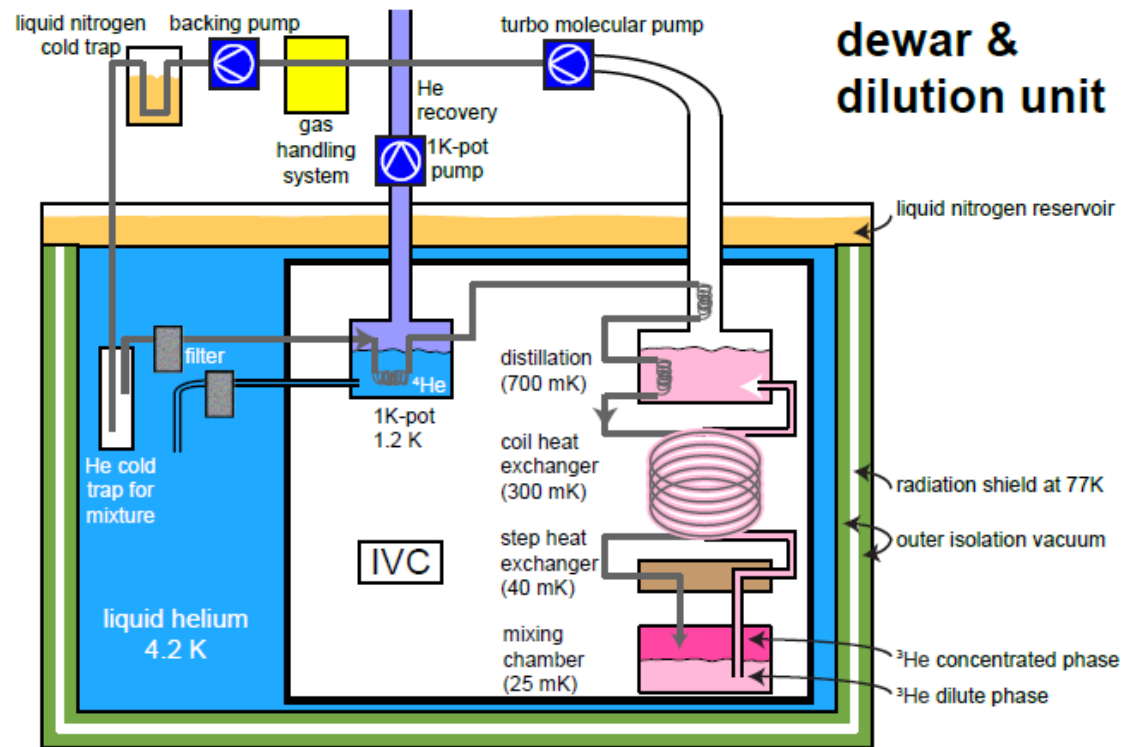
Here,  $Z = \sum_j g_j \exp(-E_j/k_B T)$  is the partition function,  $g_i$  is the degeneracy of each energy level  $E_i$ . For convenience, we set  $E_0 = 0$ .

For a “hot” 2-level system without degeneracy ( $g_i = 1$ ),  $Z=2$ , we find  $P_{|1\rangle}(T_{\text{hot}}) = 1/2$ .

In experiments, we want  $P_{|1\rangle}(T_{\text{cold}}) \ll 1\%$ . Hence, we need

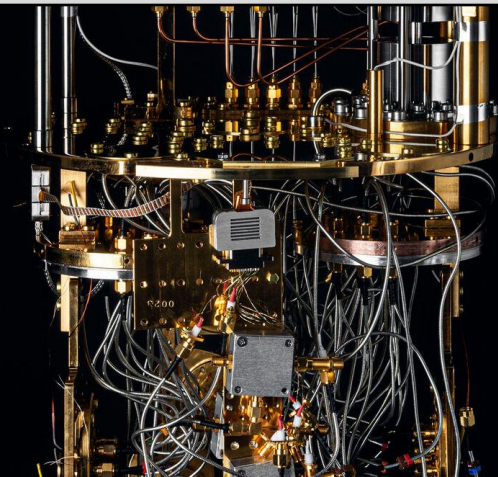
$$k_B T \ll \hbar \omega_q$$

# In the lab: cooling down a circuit

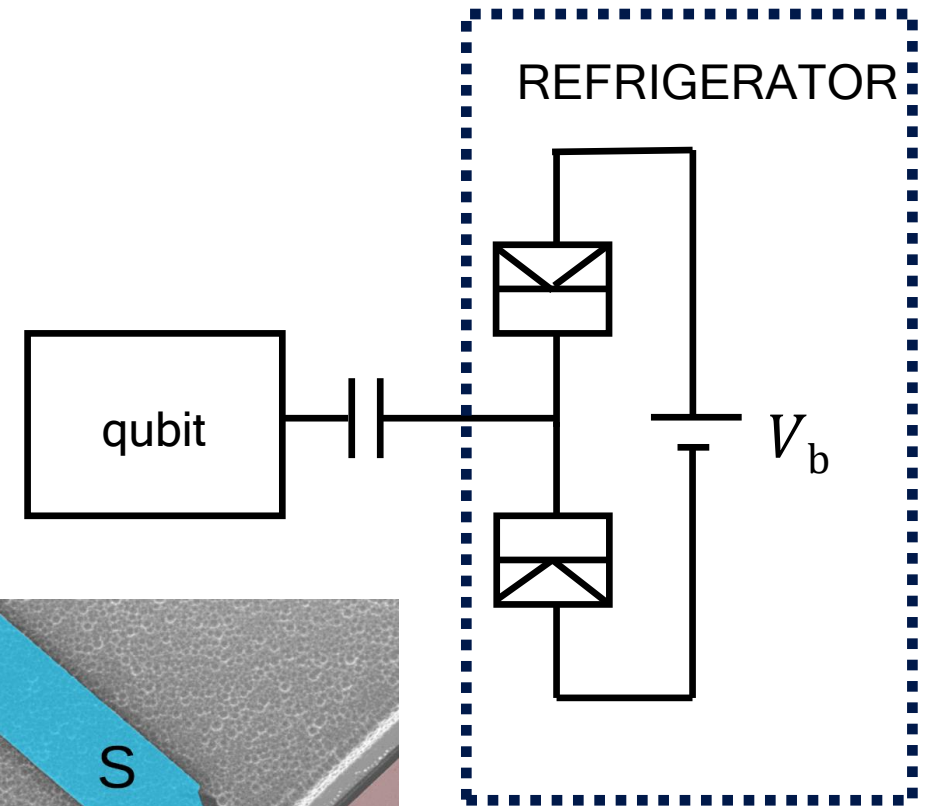
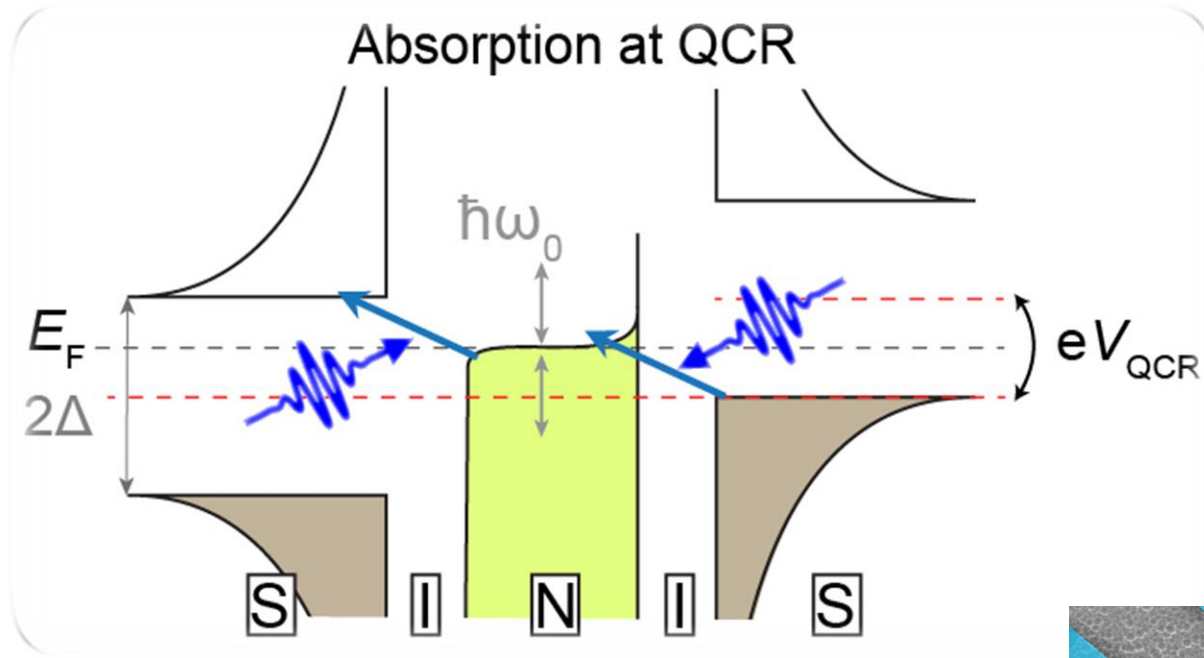


Key takeaway: Superconducting circuits need to be cooled to mK temperatures to avoid thermal excitation ( $50\text{mK} \leftrightarrow 1\text{GHz}$ ).

Initialization can be done by waiting several qubit lifetimes ( $5 T_1 \sim 0.5\text{ms}$ )

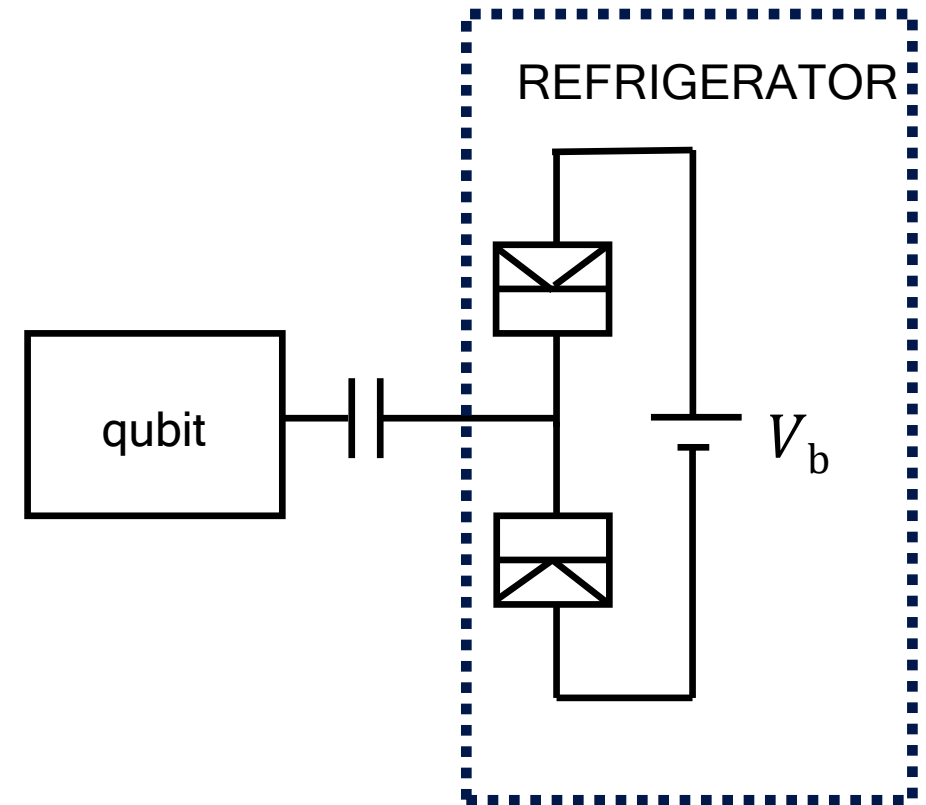
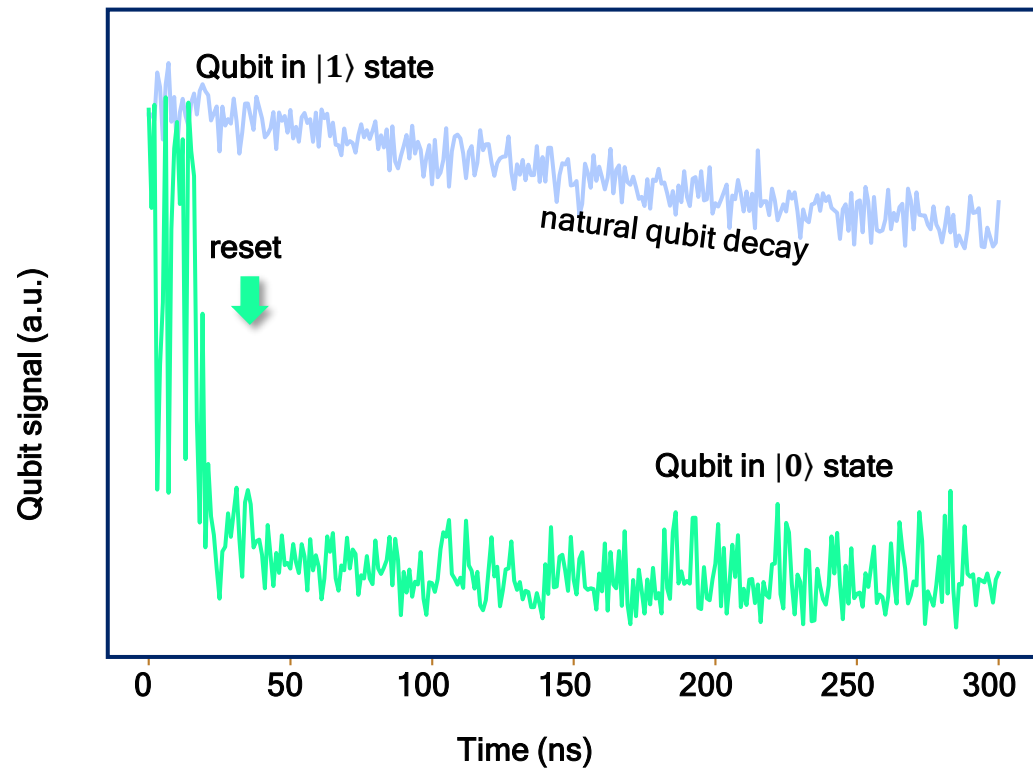


# On the chip: active cooling through a Quantum-Circuit Refrigerator (QCR)



EXPERIMENT: K.Y. Tan, *et al.*, Nat. Commun. **8**, 15189 (2017)  
THEORY: M. Silveri, *et al.*, Phys. Rev. B **96**, 094524 (2017)

# On the chip: active cooling through a Quantum-Circuit Refrigerator (QCR)



EXPERIMENT: K.Y. Tan, *et al.*, Nat. Commun. **8**, 15189 (2017)  
THEORY: M. Silveri, *et al.*, Phys. Rev. B **96**, 094524 (2017)

# More advanced: feedback-based reset

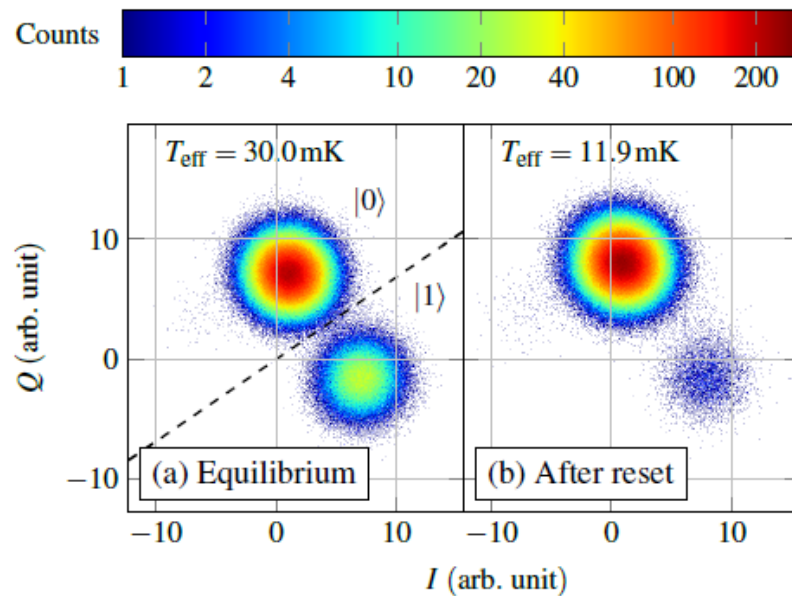
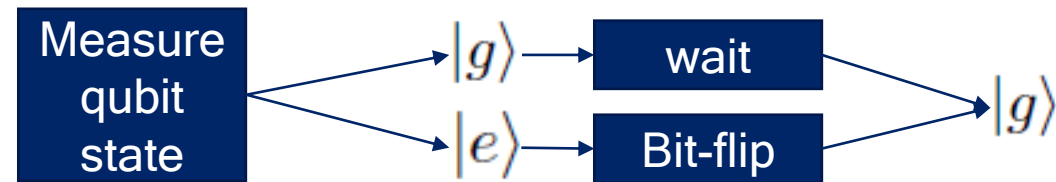


FIG. 2. Demonstration of quantum feedback by using an active reset sequence. (a) shows the cavity response before the active reset operation while the qubit is in thermal equilibrium with the environment. The linear discriminant used to determine the qubit state in real-time on our platform is indicated as dashed line. (b) shows the response directly after preparing the qubit in its ground state  $|0\rangle$  with an active reset operation.

arXiv:1912.06814v1

Instead of physical cooling, we can reduce the effective temperature of a qubit by feedback control.

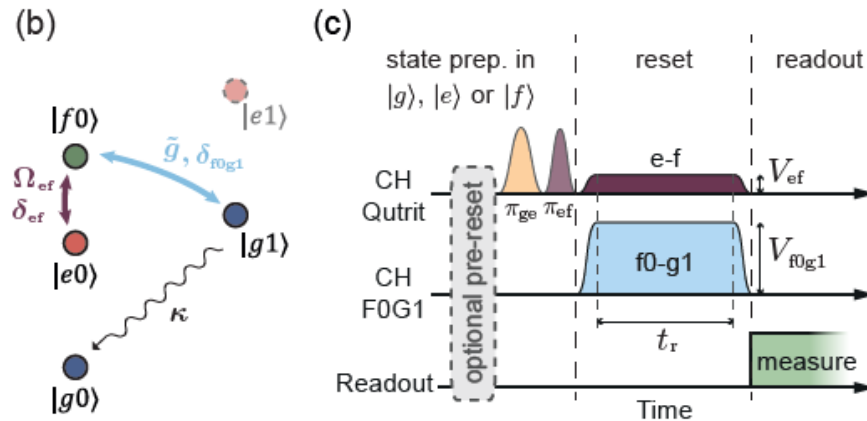


The disadvantage of this approach is the relatively long feedback cycle  $\sim 1.5 \mu\text{s}$ .

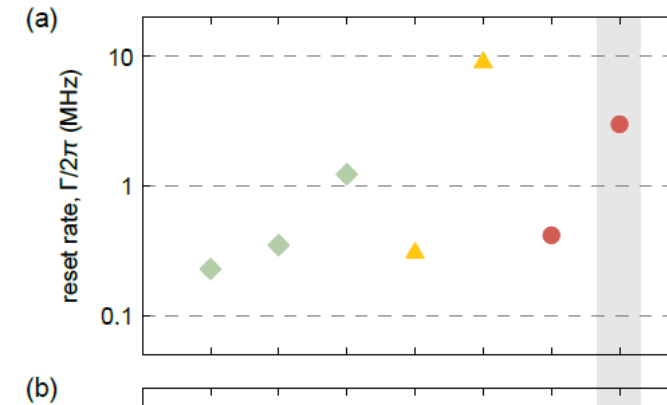
We developed a versatile integrated control and readout instrument for experiments with superconducting quantum bits (qubits), based on a field-programmable gate array (FPGA) platform. Using this platform, we perform measurement-based, closed-loop feedback operations with 428 ns platform latency. The feedback capability is instrumental in realizing active reset initialization of the qubit into the ground state in a time much shorter than its energy relaxation time  $T_1$ . We show experimental results demonstrating reset of a fluxonium qubit with 99.4 % fidelity, using a readout-and-drive pulse sequence approximately  $1.5 \mu\text{s}$  long. Compared to passive ground state initialization through thermalization, with the time constant given by  $T_1 = 80 \mu\text{s}$ , the use of the FPGA-based platform allows us to improve both the fidelity and the time of the qubit initialization by an order of magnitude.



# More advanced: unconditionally pulsed reset



The reset concept, illustrated in Fig. 1b, is based on a cavity-assisted Raman transition between  $|f, 0\rangle$  and  $|g, 1\rangle$  [29, 35, 36]. Here  $|s, n\rangle$  denotes the tensor product of the transmon in state  $|s\rangle$ , with  $|g\rangle$ ,  $|e\rangle$  and  $|f\rangle$  its three lowest energy eigenstates, and the reset resonator in the  $n$  photon Fock state  $|n\rangle$ . By simultaneously driving the  $|f, 0\rangle \leftrightarrow |g, 1\rangle$  (f0-g1) transition and the  $|e, 0\rangle \leftrightarrow |f, 0\rangle$  (e-f) transition, the population is transferred from the qutrit excited states,  $|e, 0\rangle$  and  $|f, 0\rangle$ , to the state  $|g, 1\rangle$ . The system then rapidly decays to the target dark state  $|g, 0\rangle$  by photon emission at rate  $\kappa$ , effectively resetting the qubit to its ground state.



Key takeaway: Instead of waiting, one can **actively cool the system** further (on-chip or feedback), or one can apply pulsed-base reset schemes.

Risté et al. (2012)

Campagne-Ibarcq et al. (2013)

Salathé et al. (2017)

Valenzuela et al. (2006)

Reed et al. (2010)

Geerlings et al. (2013)

This work

arXiv:1801.07689v1

# Review: Initialization

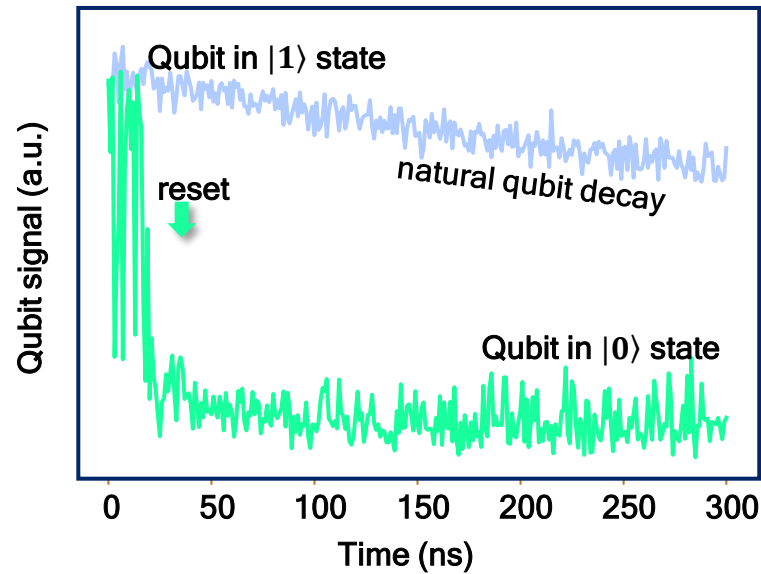
- To **start a computation**, it is necessary that all registers are in a well-known state, typically the 0-state.
- For experimental implementation, **thermal noise** always drives us out of equilibrium when approaching the 0-state.
- We can compensate this by **actively cooling** or used more advanced feedback or pulse schemes.

# Agenda for today

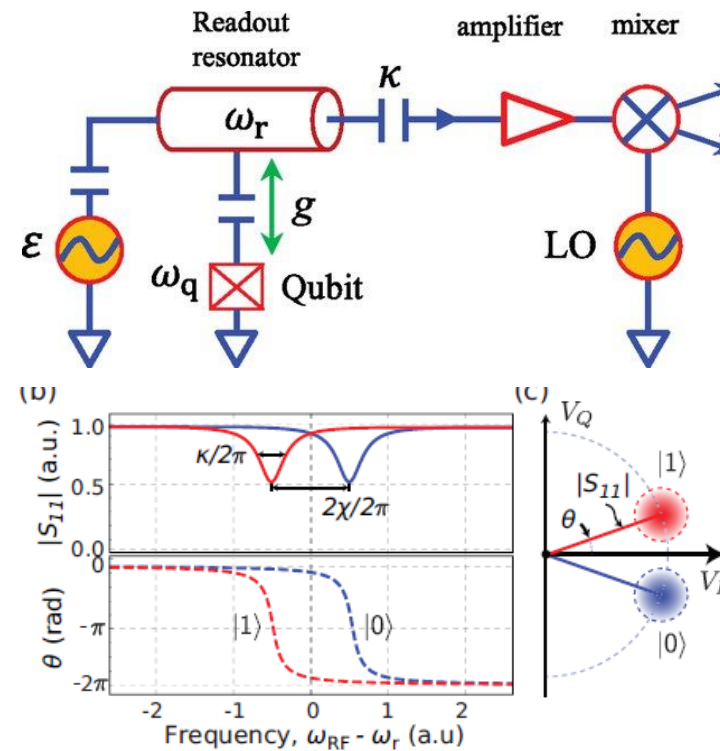
## 9. Single-qubit operations:

- Initialization **2<sup>nd</sup> DiVincenzo criteria**
- Readout **5<sup>th</sup> DiVincenzo criteria**
- Control: T1, T2 measurements, Randomized benchmarking **3<sup>rd</sup> DiVincenzo criteria**

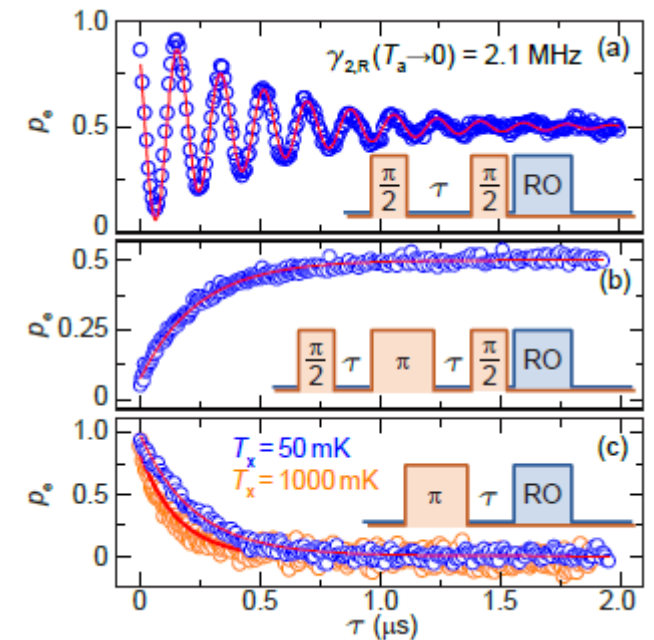
a.



b.



c.

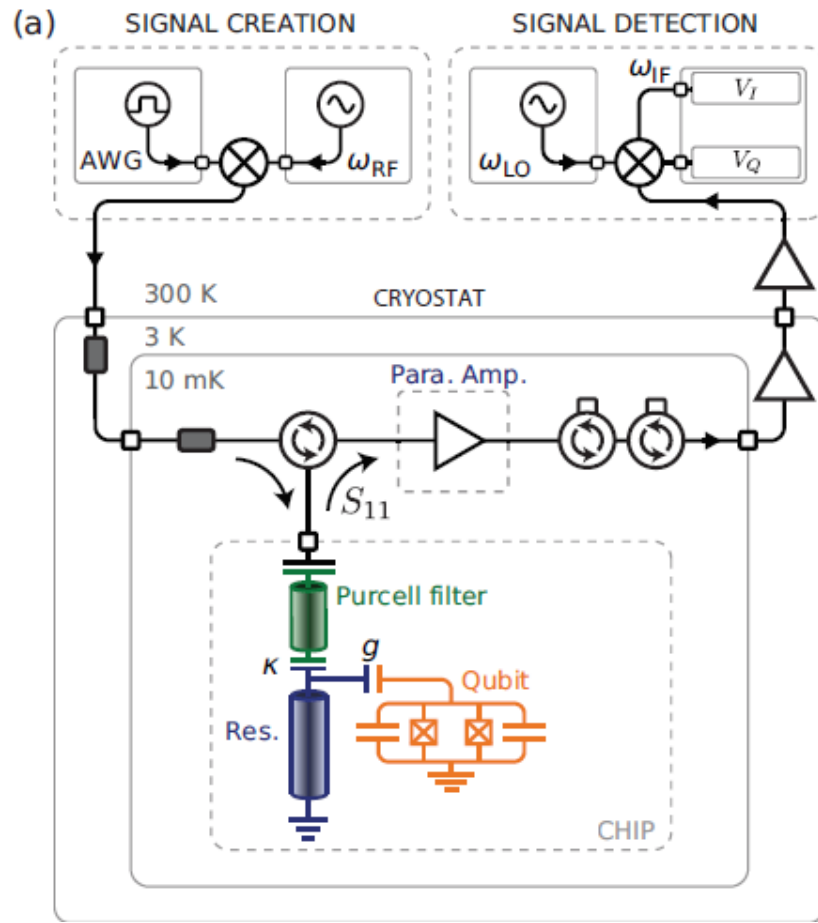




# General approach: Qubit readout

- To **determine the qubit state**, we must project it onto an eigenstate and measure the expectation value.
- Hence, measurements must be **averaged many times** to distill the relevant probability distribution.
- We don't read out the qubit directly but use the interaction with a superconducting resonator. This allows us to perform **single-shot qubit readout**.

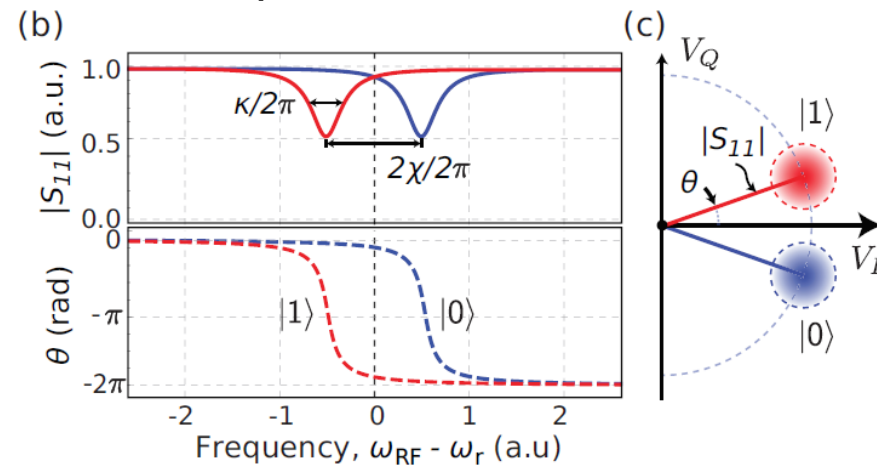
# Dispersive readout of qubits



We consider a qubit strongly coupled to a resonator in the dispersive limit of the Jaynes-Cummings model:

$$H_{\text{disp}} = \left( \omega_r + \chi \sigma_z \right) \left( a^\dagger a + \frac{1}{2} \right) + \frac{\tilde{\omega}_q}{2} \sigma_z$$

Where  $\chi = g^2/\Delta$  is the qubit-state dependent frequency shift, a so-called *dispersive shift*.



The phase shift can be detected either by recording a complete spectrum or as single shot.

# Time-resolved readout of qubits

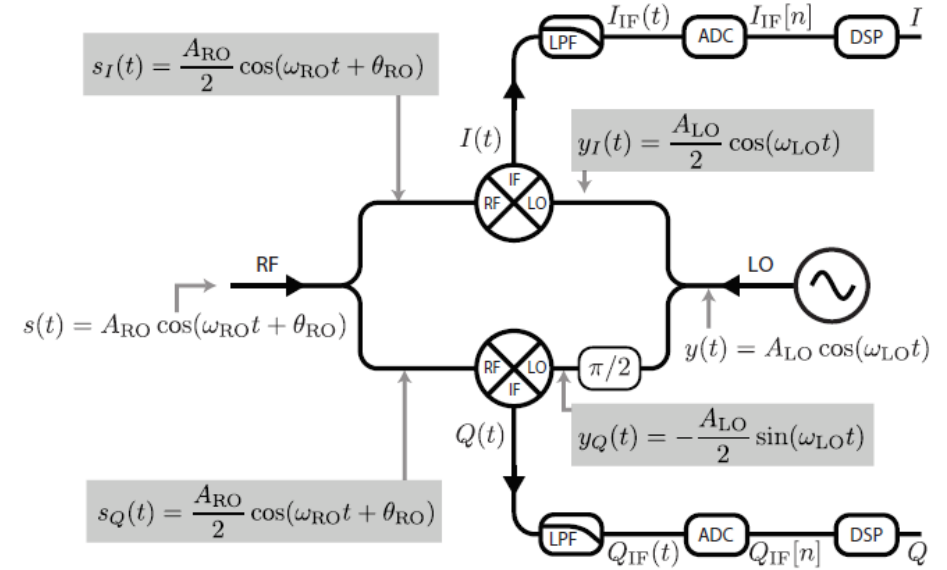
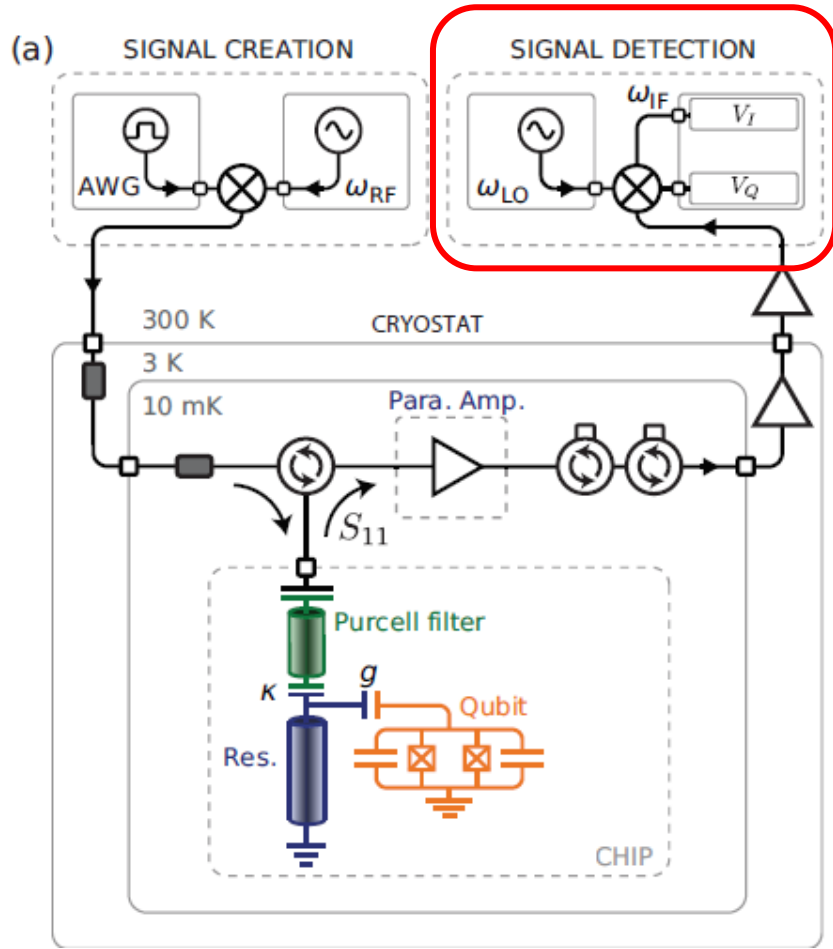


FIG. 21. Schematic of an I-Q mixer. A readout pulse at frequency  $\omega_{RO}$  enters the RF port, where it is equally split into two paths. A local oscillator at frequency  $\omega_{LO}$  enters the LO port, where it is equally split into two paths, one of which undergoes a  $\pi/2$ -radian phase rotation. To perform analog modulation, the two signals in each path are multiplied at a mixer, yielding the outputs  $I(t)$  and  $Q(t)$ , each having frequencies  $\omega_{RO} \pm \omega_{LO}$ .  $I(t)$  and  $Q(t)$  are then low-pass-filtered (time averaged) to yield  $I_{IF}(t)$  and  $Q_{IF}(t)$  at the intermediate frequency  $\omega_{IF} = |\omega_{RO} - \omega_{LO}|$ , and subsequently digitized using an analog-to-digital (ADC) converter. If  $\omega_{IF} \neq 0$ , then digital signals  $I_{IF}[n]$  and  $Q_{IF}[n]$  are further digitally demodulated using digital signal processing (DSP) techniques to extract the amplitude and phase of the readout signal.

# Time-resolved readout of qubits

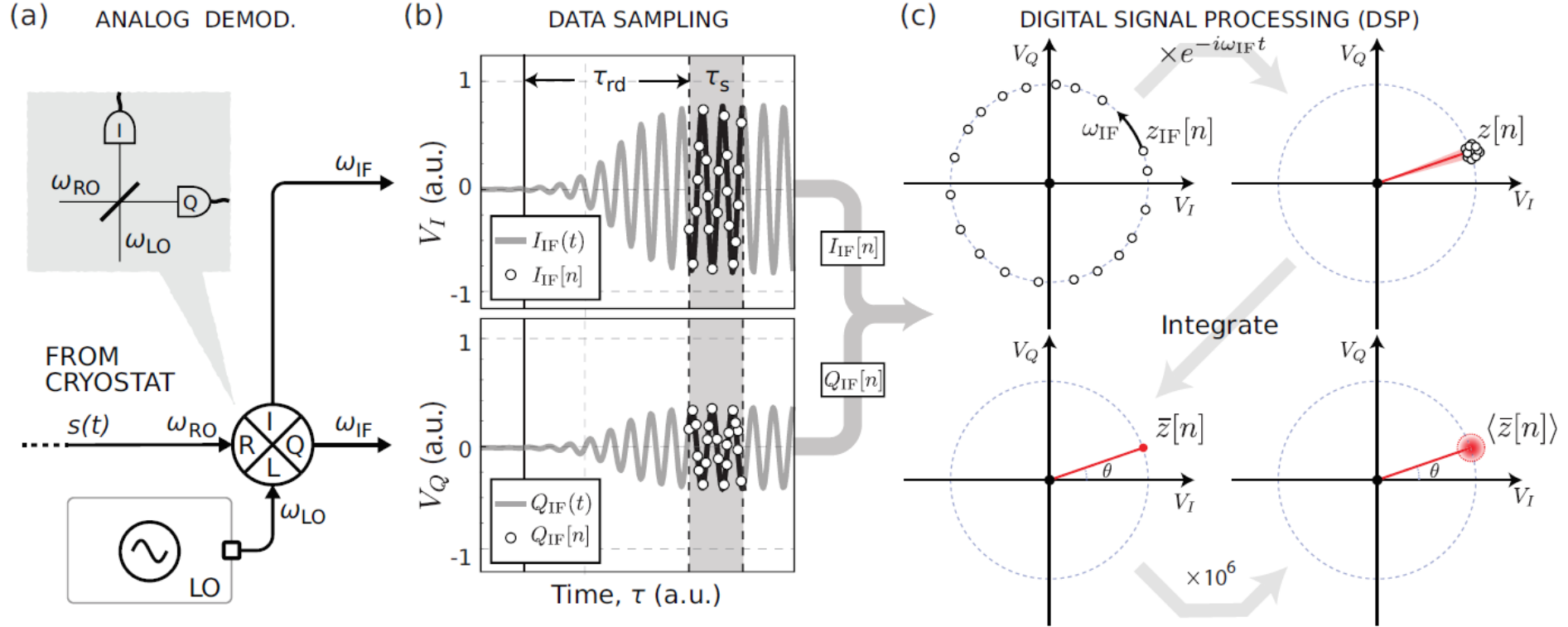
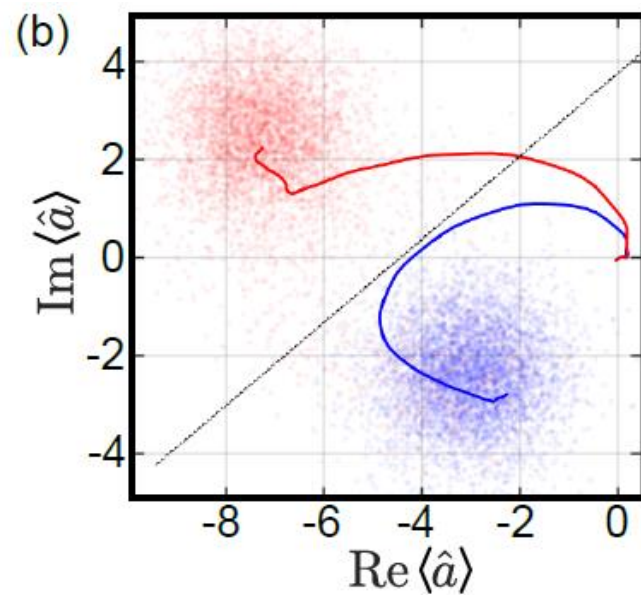
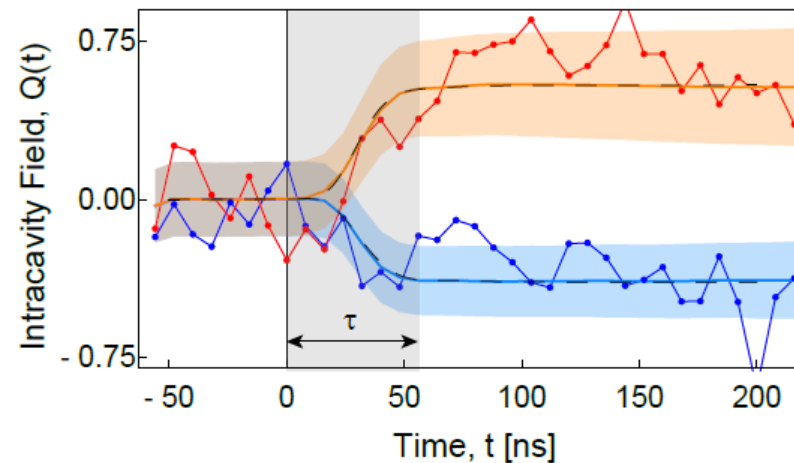
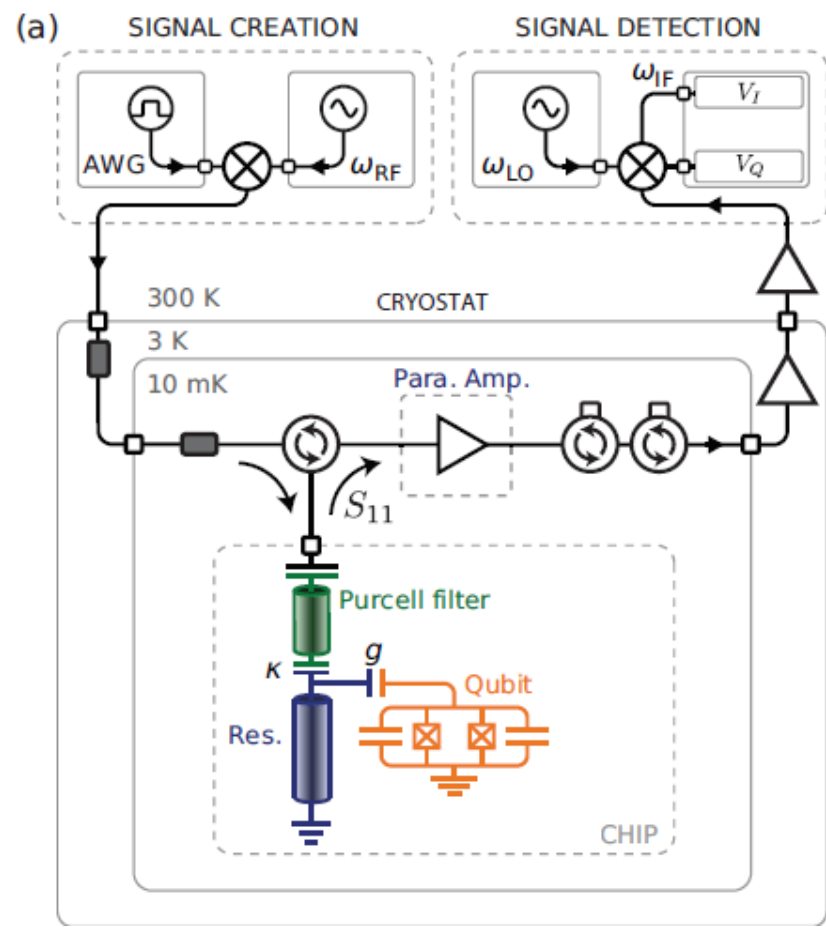


FIG. 22. Schematic of the heterodyne detection technique. (a) The signal with frequency  $\omega_{RF}$  from the cryostat is mixed with a carrier tone with frequency  $\omega_{LO}$ , yielding two quadratures at a down-converted intermediate frequency  $\omega_{IF} = |\omega_{RO} - \omega_{LO}|$ , and  $90^\circ$  out-of-phase with each other. (b) The two signals are passed into two different analog-to-digital converter (ADC) channels. To avoid sampling the resonator transient, some readout delay ( $\tau_{rd}$ ) corresponding to the resonator linewidth may be added, and the two signals are sampled for a time  $\tau_s$ . In this case, the white dots represent the sampled points. (c) The sampled traces are post-processed and after some algebra, the sampled data points are averaged into a single point in the  $(I, Q)$ -plane. To extract statistics of the readout performance, i.e. single-shot readout fidelity, a large number of  $(I, Q)$ -records are acquired, yielding a 2D-histogram, with a Gaussian distributed spread given by the noise acting on the signal.

# Single shot readout of qubits



Key takeaway: Qubit readout is done through a resonator and can be achieved in less than 100ns for a single shot approach.

# Review: Qubit readout

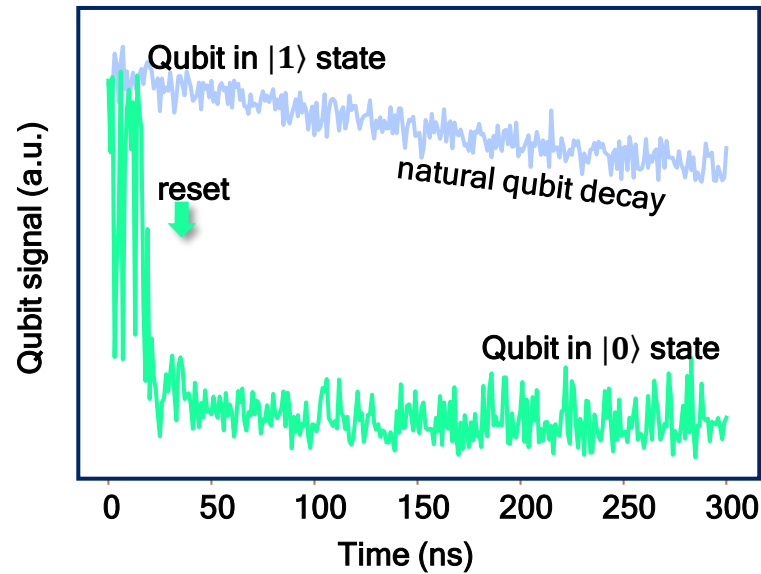
- To **determine the qubit state**, we must project it onto an eigenstate and measure the expectation value.
- Hence, measurements must be **averaged many times** to distill the relevant probability distribution.
- We don't read out the qubit directly but use the interaction with a superconducting resonator. This allows us to perform **single-shot qubit readout**.

# Agenda for today

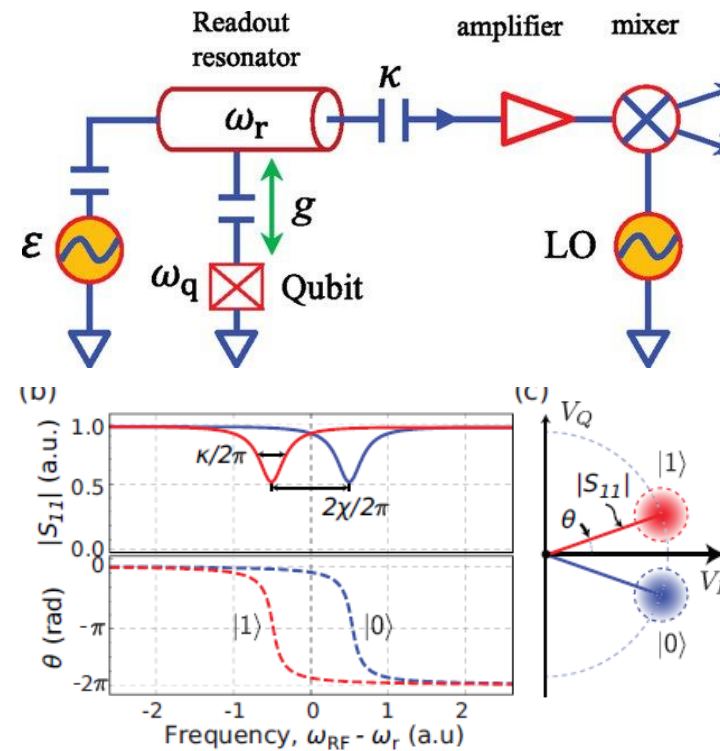
## 9. Single-qubit operations:

- Initialization **2<sup>nd</sup> DiVincenzo criteria**
- Readout **5<sup>th</sup> DiVincenzo criteria**
- Control: T1, T2 measurements, Randomized benchmarking **3<sup>rd</sup> DiVincenzo criteria**

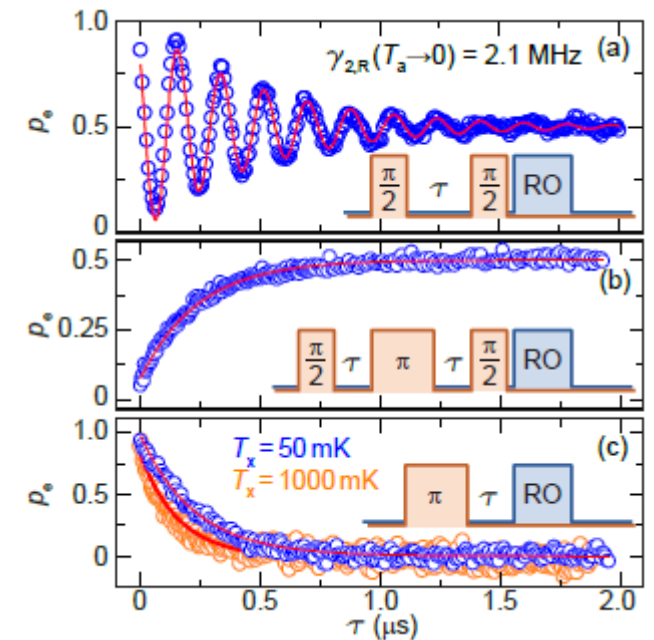
a.



b.



c.



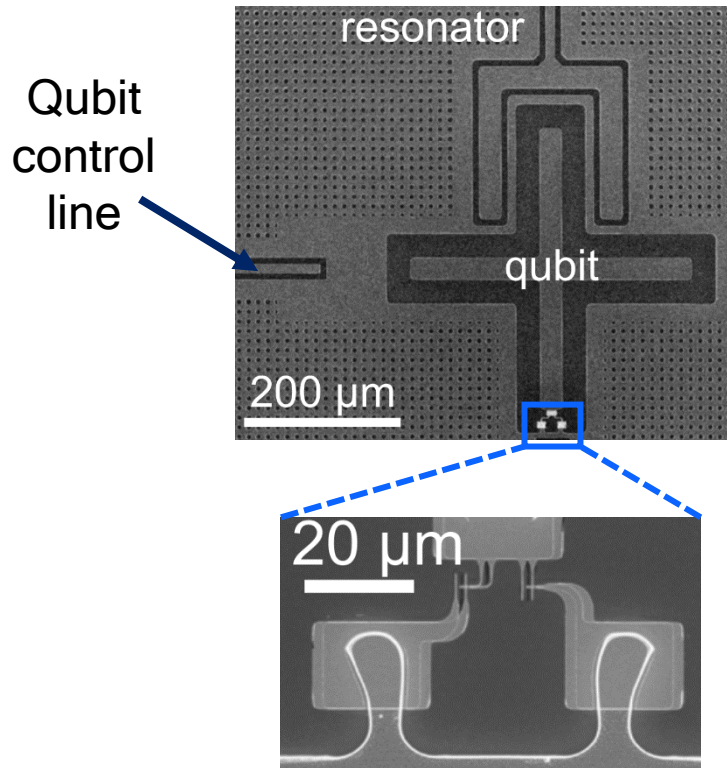


# General approach: Qubit control

- To **determine the qubit state**, we must project it onto an eigenstate and measure the expectation value.
- Hence, measurements must be **averaged many times** to distill the relevant probability distribution.
- We don't read out the qubit directly but use the interaction with a superconducting resonator. This allows us to perform **single-shot qubit readout**.



# Controlling the qubit state through MW pulses



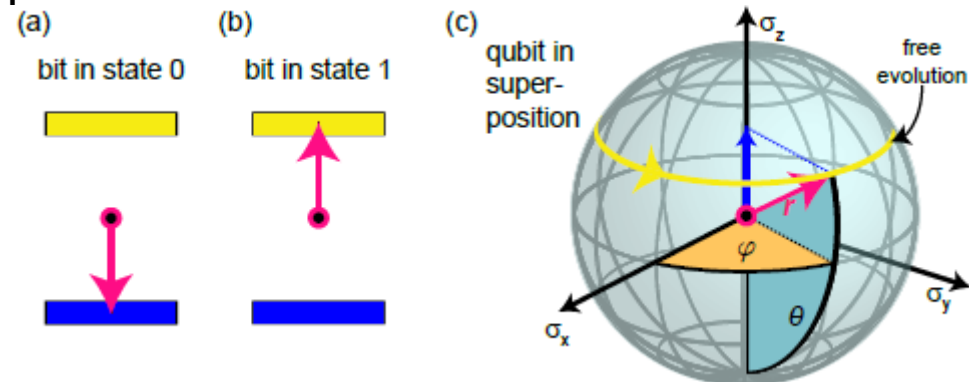
To control the qubit state, we use an on-chip control line and apply coherent microwave signals. They add an energy term to the Hamiltonian:

$$\mathcal{H}_{d,q} = \frac{\hbar}{2} [\omega_q \hat{\sigma}_z + 2\Omega_d \cos(\omega_d t) \hat{\sigma}_x]$$

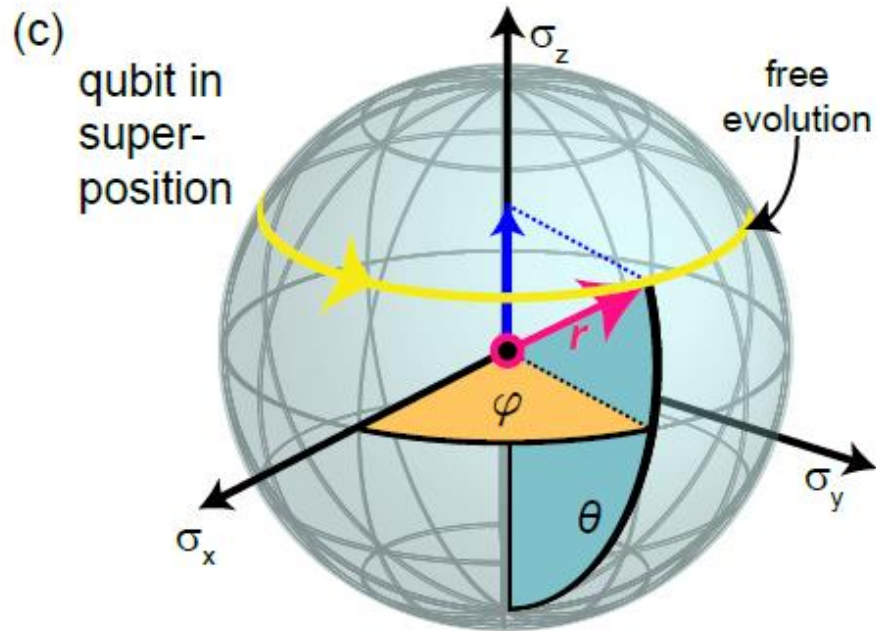
Using a unitary transformation, we can bring this Hamiltonian into the following form:

$$\mathcal{H}'_d = \hbar\Omega_R \hat{\sigma}_x$$

Hence, we can rotate the state vector about the x-axis in this way. We can apply rotations about the y-axis by introducing a finite phase to the drive.



# Non-resonant driving



**Non-resonant driving** For a non-resonant drive with detuning  $\delta_d = \omega_q - \omega_d$ , we transform into a frame rotating with the drive frequency  $\omega_d$ . That way, the time-independent interaction Hamiltonian in a rotating wave approximation can be expressed as  $\mathcal{H}'_d = \hbar[\delta_d \hat{\sigma}_z + \Omega_d \hat{\sigma}_x]/2$ . This Hamiltonian shows that the rotation frequency changes to  $\Omega_R^* = \sqrt{\Omega_R^2 + \delta_d^2}$

(2.1.4)

# Non-resonant driving

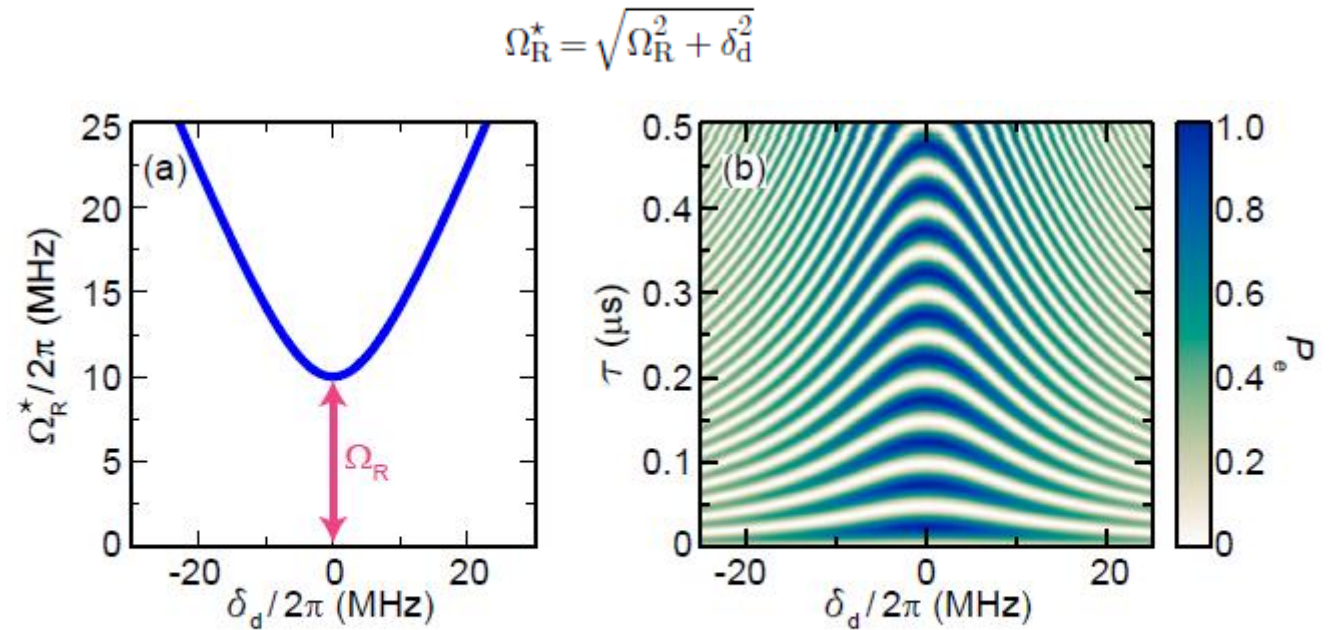
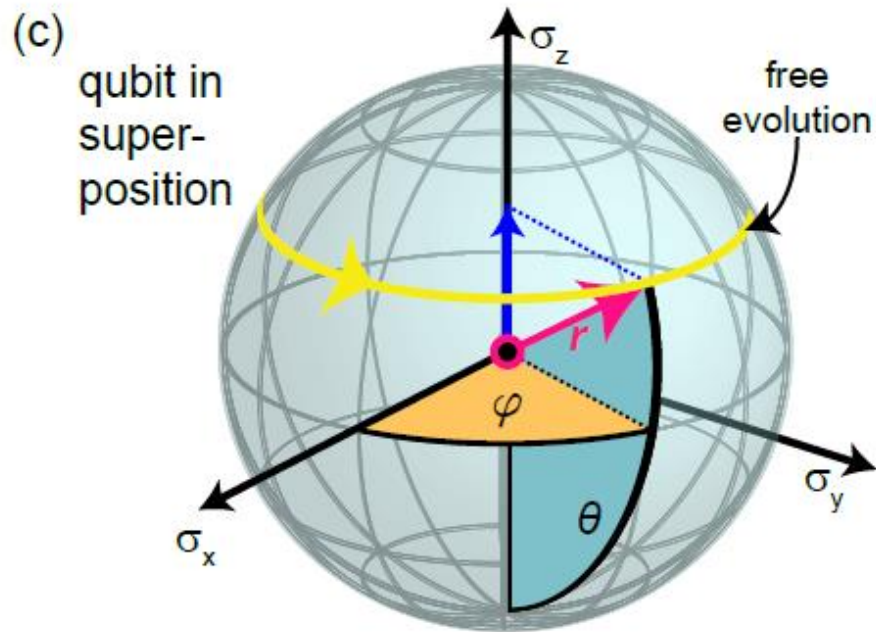


**Figure 2.2:** (a) Effective Rabi frequency  $\Omega_R^*$  plotted versus detuning  $\delta_d$  for  $\Omega_R = 10$  MHz. (b) Excited state probability in the absence of decoherence plotted versus detuning  $\delta_d$  and pulse duration  $\tau$ .

# Experimental determination of $\pi$ & $\pi/2$ pulses

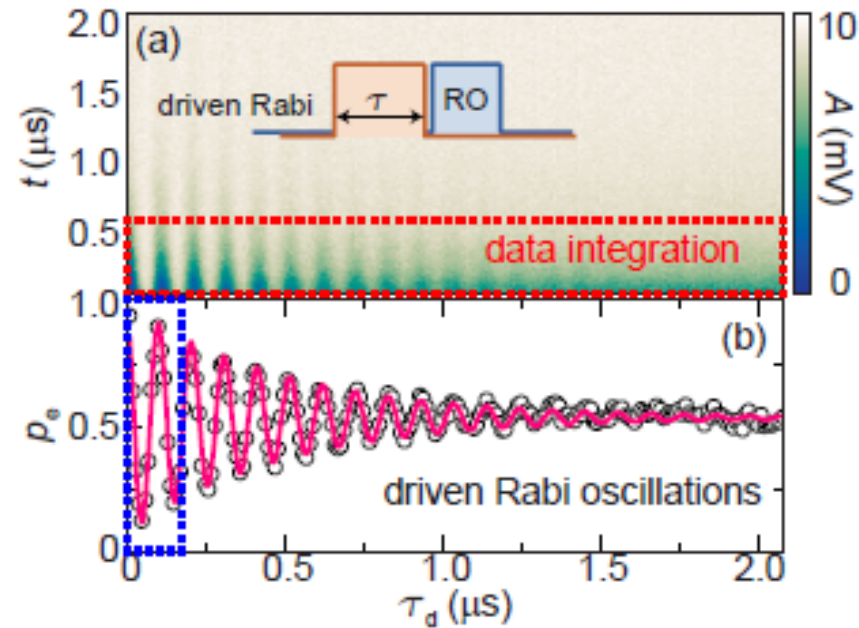
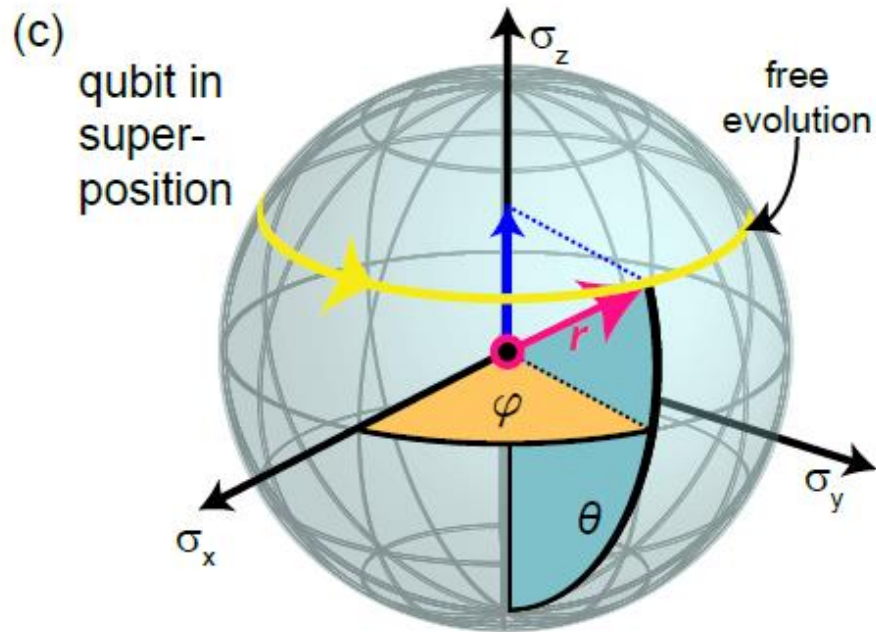
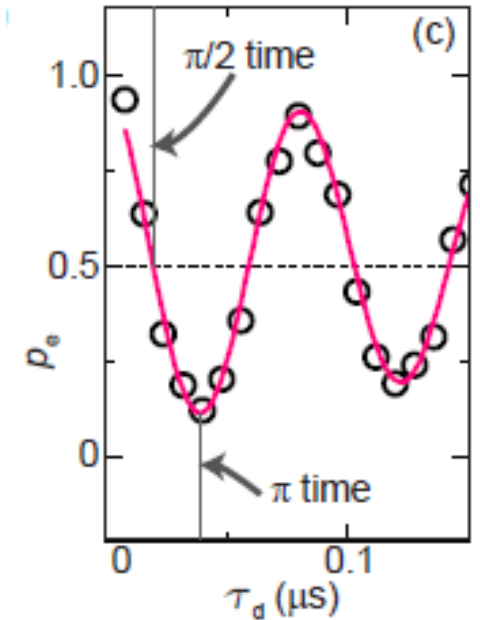
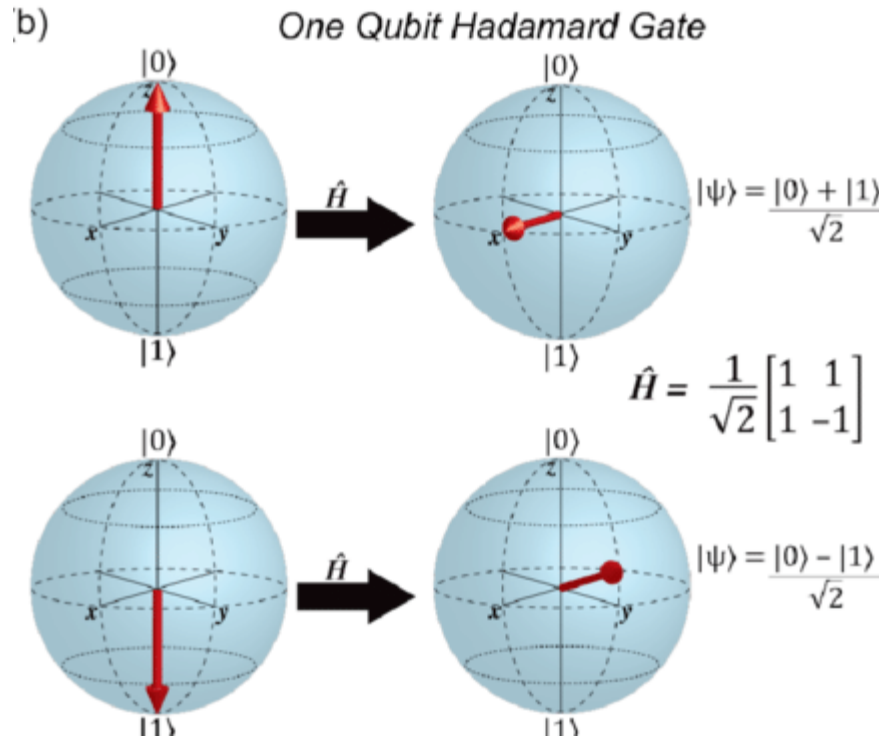
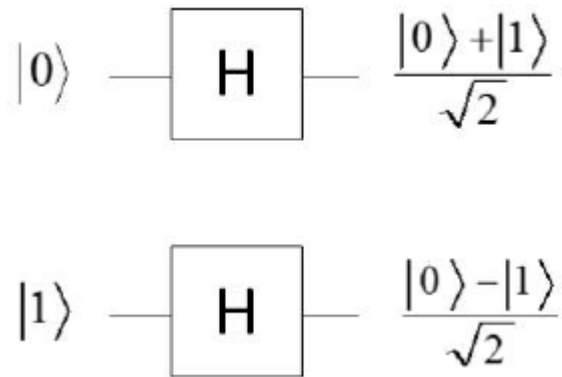


**Figure 4.34:** (a) Transmission amplitude (color code) plotted versus time and pulse duration in a pulsed driven Rabi experiment. For the analysis of the excited state probability, we take only data points from the area highlighted by the red dashed rectangle into account. (b) Excited state probability plotted versus pulse duration for the data shown in (a). (c) Zoom into the blue dashed rectangle in panel (b) to illustrate the  $\pi/2$  and the  $\pi$  time.

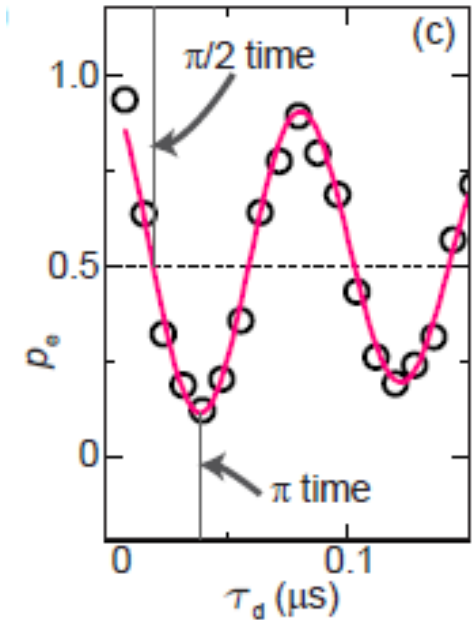


# $\pi/2$ pulses: The Hadamard gate

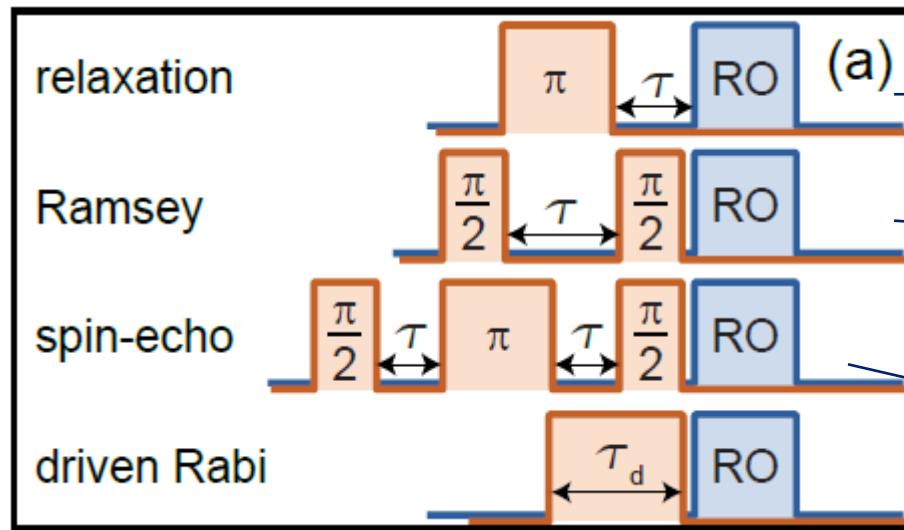


# Other single-qubit gates

Operator	Gate(s)	Matrix
Pauli-X (X)	$\boxed{\text{X}}$ $\oplus$	$\begin{bmatrix} 0 & 1 \\ 1 & 0 \end{bmatrix}$
Pauli-Y (Y)	$\boxed{\text{Y}}$	$\begin{bmatrix} 0 & -i \\ i & 0 \end{bmatrix}$
Pauli-Z (Z)	$\boxed{\text{Z}}$	$\begin{bmatrix} 1 & 0 \\ 0 & -1 \end{bmatrix}$
Hadamard (H)	$\boxed{\text{H}}$	$\frac{1}{\sqrt{2}} \begin{bmatrix} 1 & 1 \\ 1 & -1 \end{bmatrix}$
Phase (S, P)	$\boxed{\text{S}}$	$\begin{bmatrix} 1 & 0 \\ 0 & i \end{bmatrix}$
$\pi/8$ (T)	$\boxed{\text{T}}$	$\begin{bmatrix} 1 & 0 \\ 0 & e^{i\pi/4} \end{bmatrix}$



# Coherence measurements



The dynamics of quantum two-level systems or qubits can conveniently be described within the Bloch-Redfield theory introducing the longitudinal relaxation (depolarization) rate

$$\gamma_1/2\pi = T_1^{-1}$$

and the transverse relaxation (dephasing) rate

$$\gamma_2/2\pi = T_2^{-1}$$

The dephasing process itself is a combination of energy decay and pure dephasing (homogeneous broadening), which obey

$$\gamma_2 = \frac{\gamma_1}{2} + \gamma_\varphi$$

characterized by the pure dephasing rate  $\gamma_\varphi$ .

# Coherence measurements: Energy relaxation

When measuring the qubit energy relaxation time, we get insights about the noise spectral density at the qubit frequency

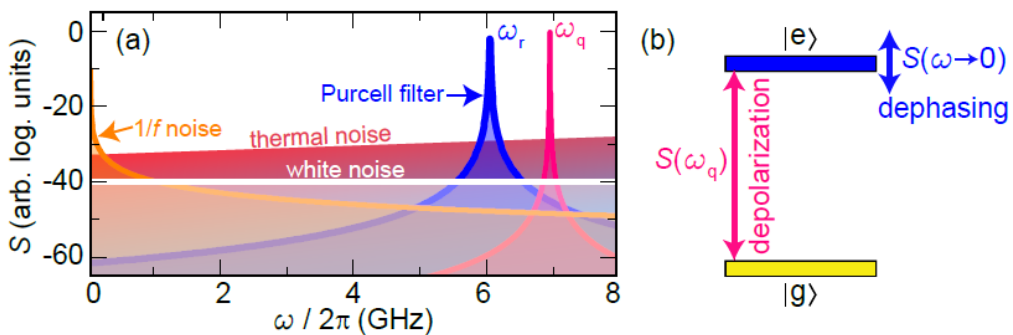
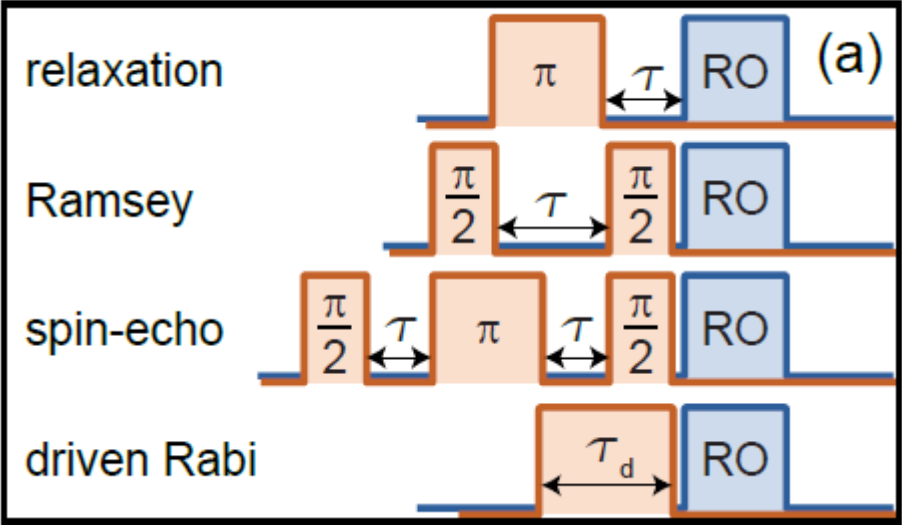
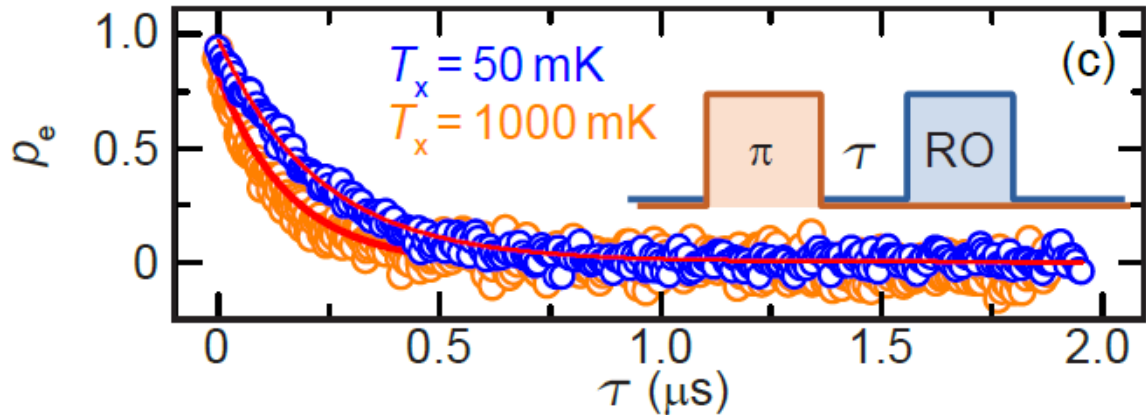
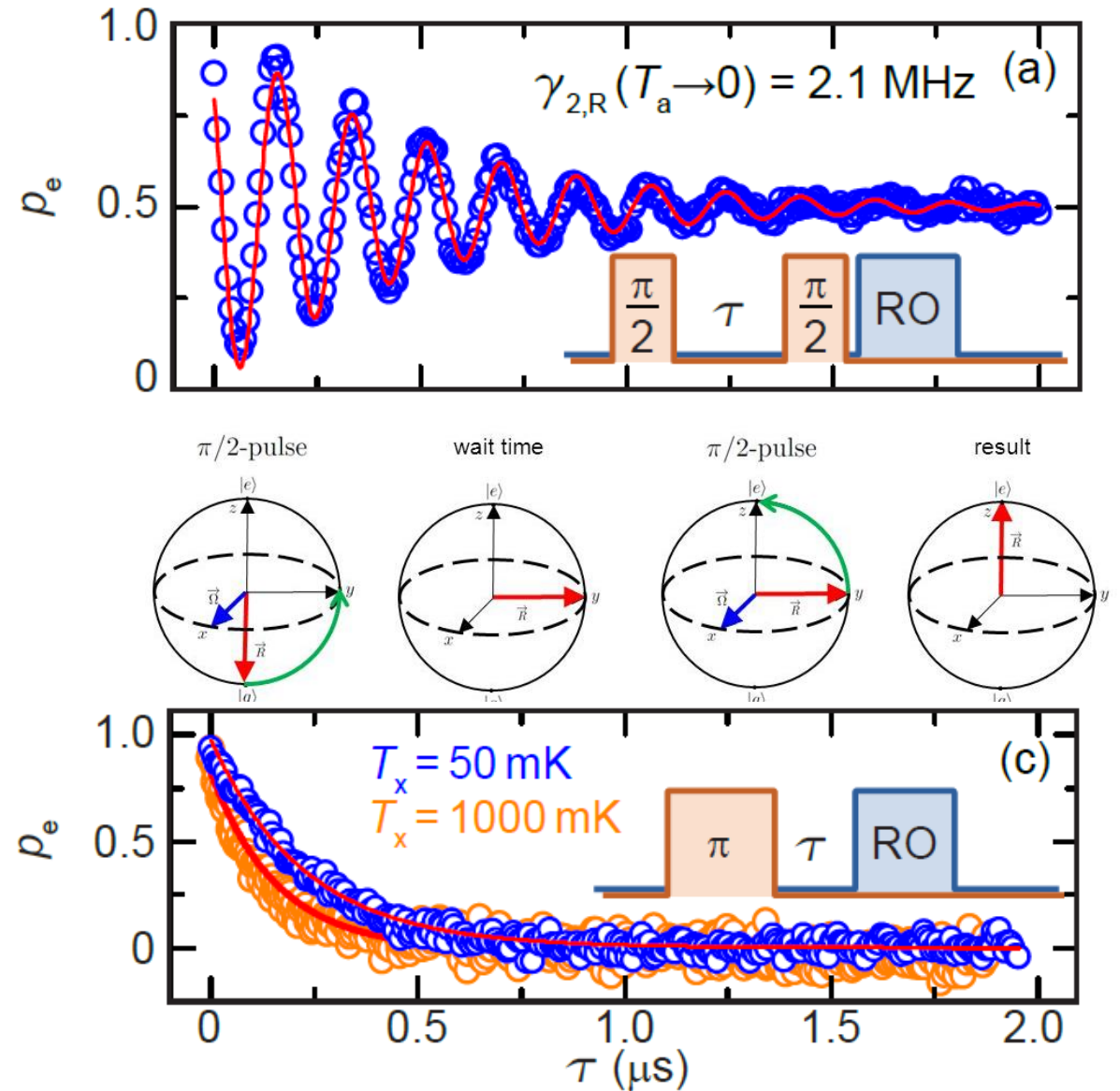
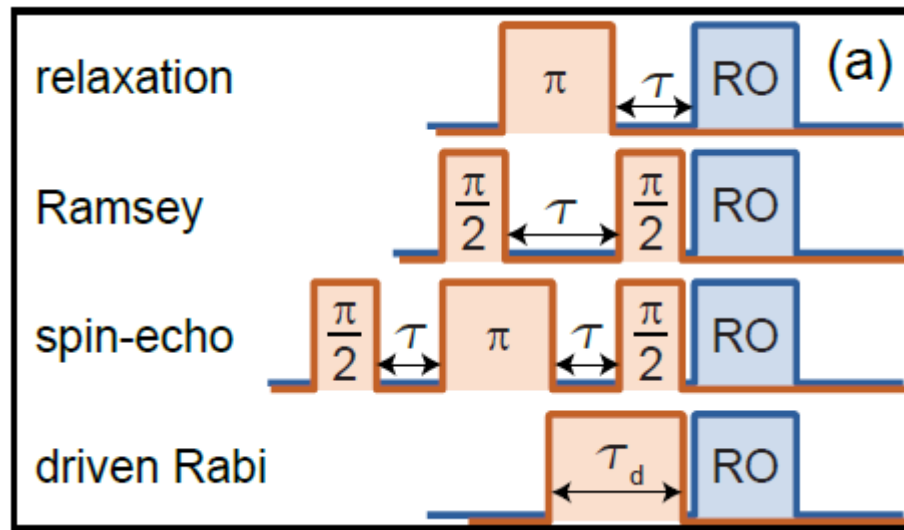


**Figure 2.29:** (a) Power spectral density for different noise sources and a Purcell filter plotted versus frequency. Additionally, we show the Lorentzian line shape of the qubit. (b) Level diagram of a qubit. A finite power spectral density  $S(\omega_q)$  at the qubit frequency introduces depolarization, while pure dephasing is caused by a spectral density  $S(\omega \rightarrow 0)$  in the low-frequency limit.

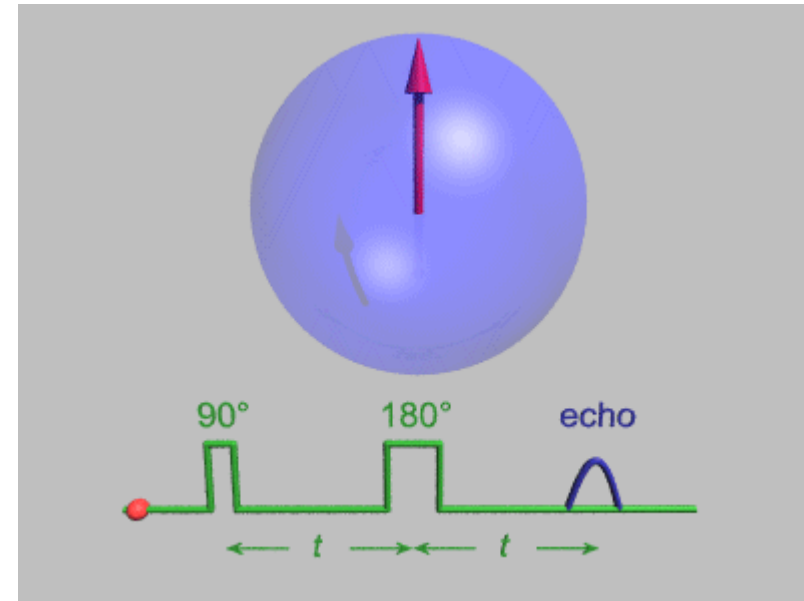
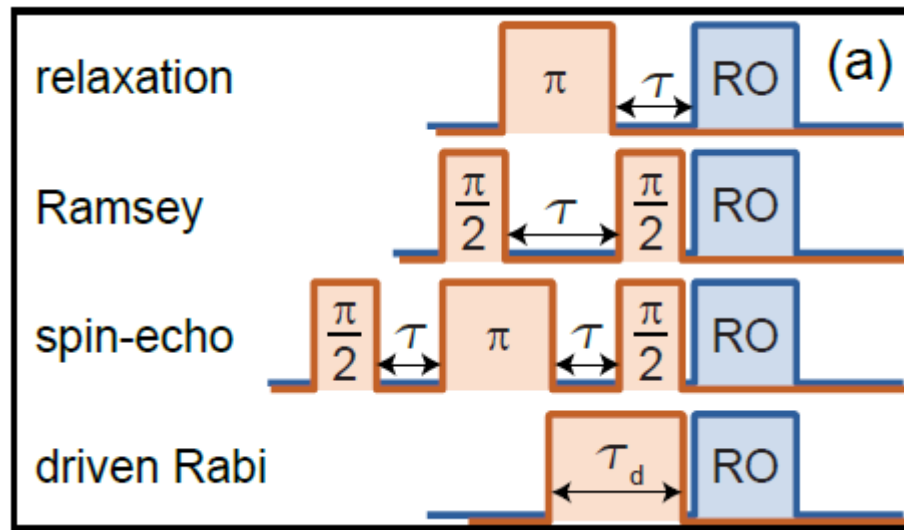




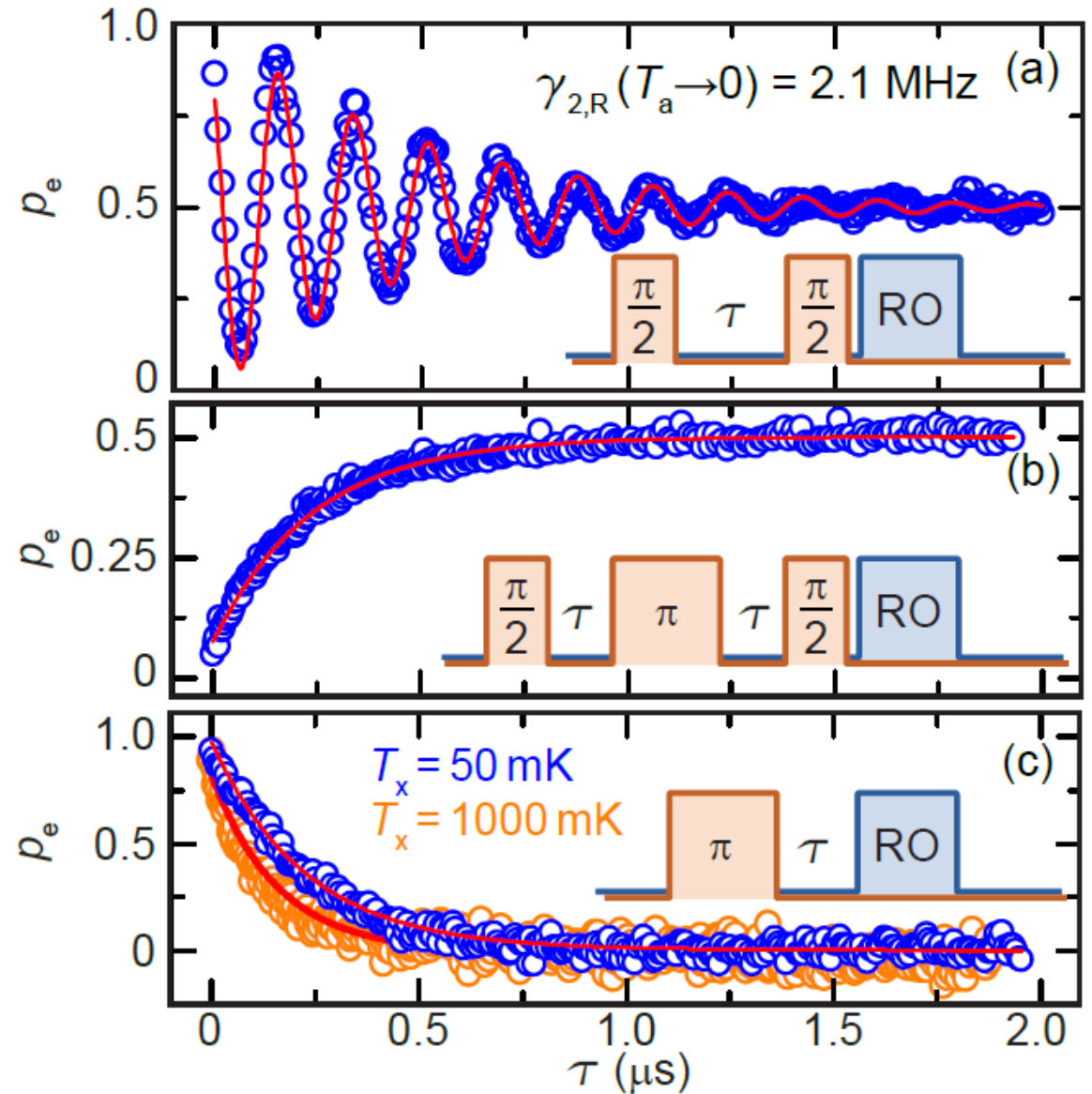
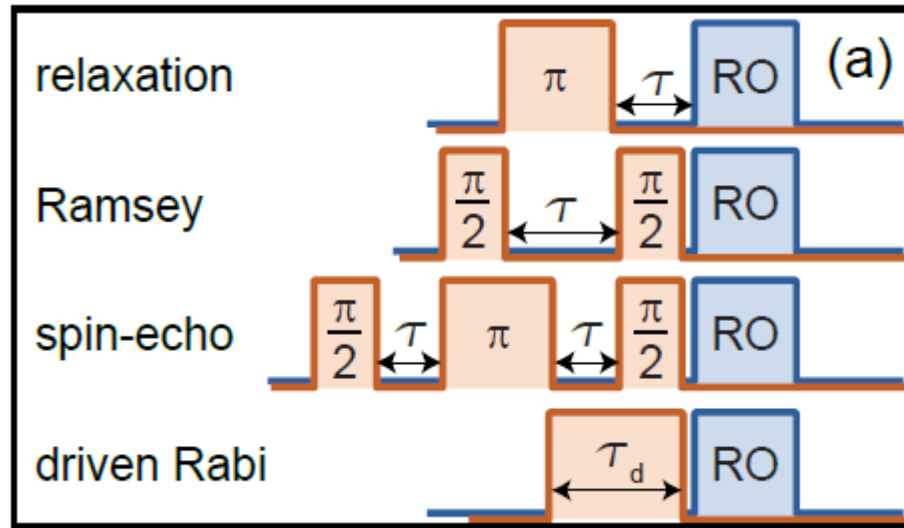
# Coherence measurements: Ramsey



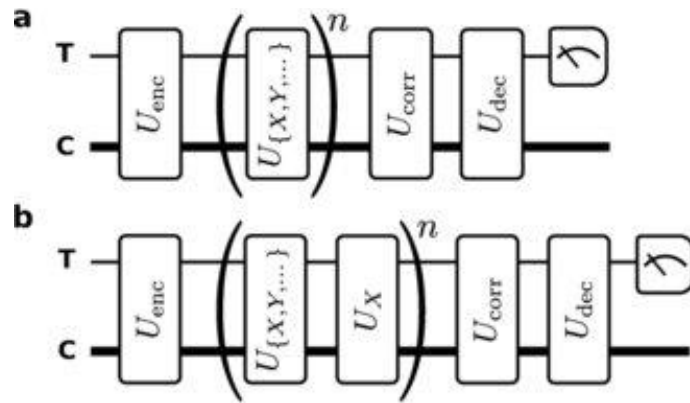
# Coherence measurements: Spin-Echo



# Coherence measurements: Spin Echo



# Coherence measurements: Randomized Benchmarking



Randomized benchmarking of operations on encoded qubit. a, Randomized benchmarking (RB) sequence.

In RB a sequence of Clifford operations of length  $n$  is chosen at random ( $U_{\{X,Y,\dots\}}$ ), followed by the operation which inverts the effect of the sequence ( $U_{corr}$ ).

To benchmark the fidelity of a certain gate  $U_x$  (for example a  $\pi$ -pulse), this gate is inserted into the gate sequence and the same analysis is performed.

By comparing the results with and with  $U_x$ , one can extract the error rate that this particular gate introduces.

# Review: Qubit control

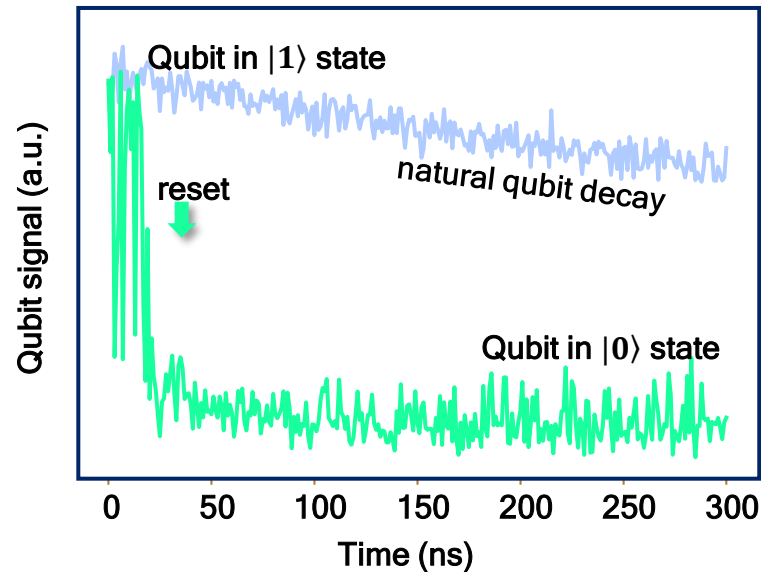
- To **determine the qubit state**, we must project it onto an eigenstate and measure the expectation value.
- Hence, measurements must be **averaged many times** to distill the relevant probability distribution.
- We don't read out the qubit directly but use the interaction with a superconducting resonator. This allows us to perform **single-shot qubit readout**.

# Agenda for today

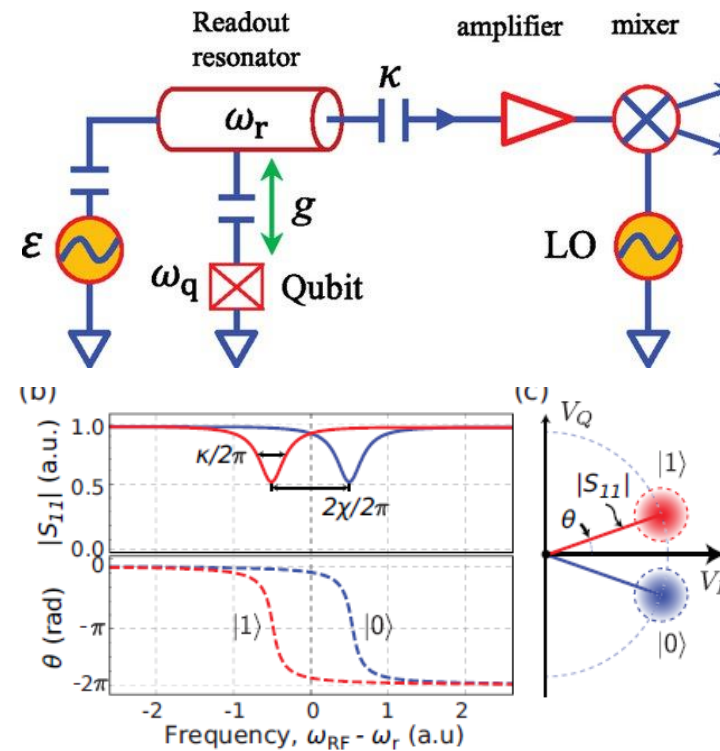
## 9. Single-qubit operations:

- Initialization 2<sup>nd</sup> DiVincenzo criteria
- Readout 5<sup>th</sup> DiVincenzo criteria
- Control: T1, T2 measurements, Randomized benchmarking 3<sup>rd</sup> DiVincenzo criteria

a.



b.



c.

